1992 CEDAR Workshop
Boulder, CO
June 21-26, 1992

Tutorial Lecture

by Michael Lockwood
Rutherford-Appleton Laboratory

Time-Varying Convection

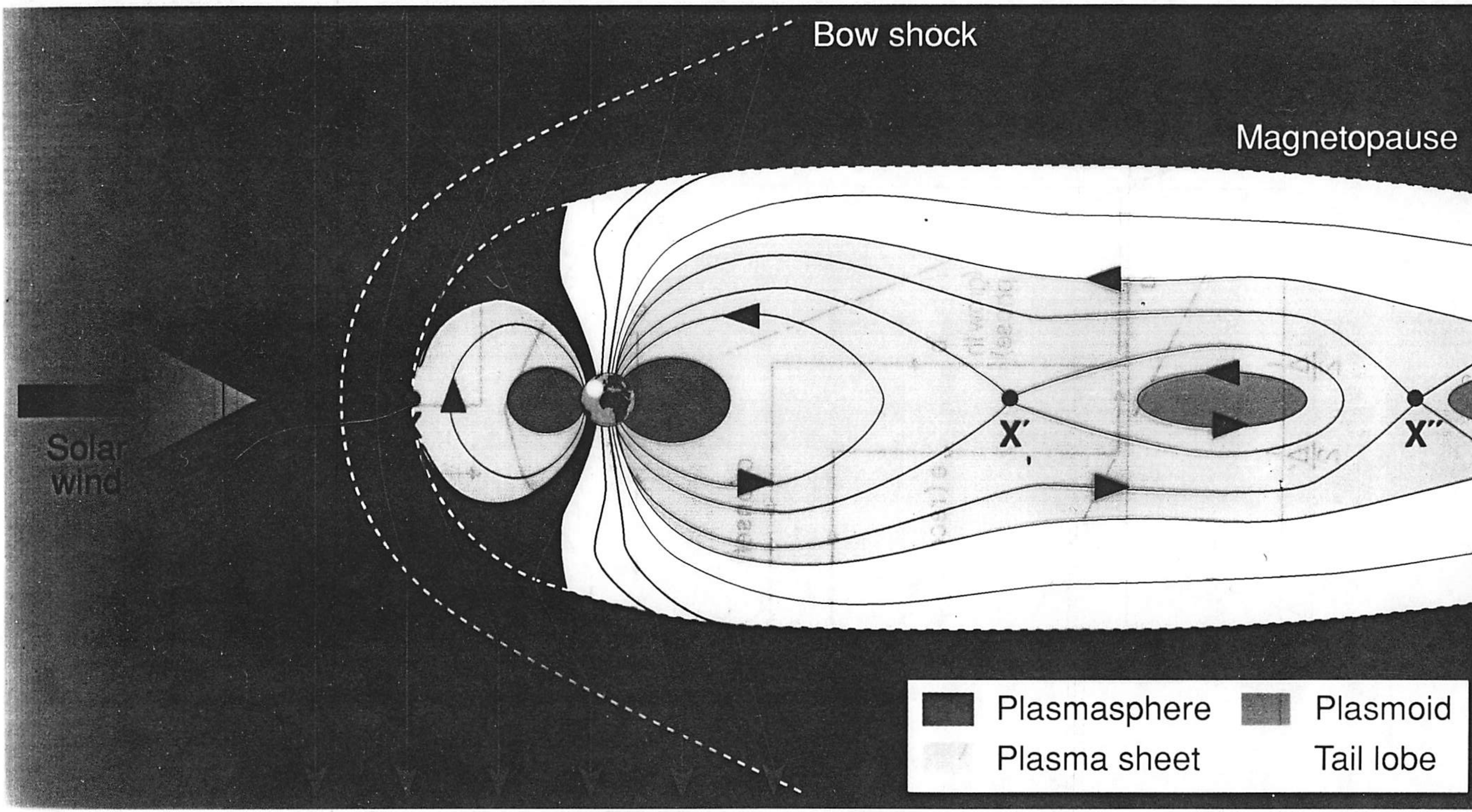
Bow shock
Magnetopause
Solar wind
X′
X″
Plasmasphere
Plasmoid
Plasma sheet
Tail lobe

Magnetohydrodynamics (MHD)

From 3 of Maxwell's equations:

$$\boxed{\begin{array}{l} \nabla . \bar{B} = 0 \\ \bar{J} = (\nabla \times \bar{B})/\mu_0 \\ \partial \bar{B}/\partial t = -(\nabla \times \bar{E}) \end{array}}$$

(Ampère's Law with $\partial D/\partial t = 0$)
(Faraday's Law)

Plus a generalised Ohm's Law

$$\boxed{\bar{J} = \sigma(\bar{E}') = \sigma(\bar{E} + \bar{v} \times \bar{B})}$$

We get the "INDUCTION EQUATION"

$$\boxed{\partial B/\partial t = \underbrace{\nabla \times (\bar{v} \times \bar{B})}_{\text{convective term}} + \underbrace{\nabla^2 B/\mu_0 \sigma}_{\text{diffusive term}}}$$

Magnetic Reynolds Number,

$$R_m = \frac{\text{convective term}}{\text{diffusive term}} \sim \frac{VB/L}{B/\mu_0 \sigma L^2} = \mu_0 \sigma V L$$

- If conductivity σ, and spatial scale, L, very large, R_m v. large $\partial B/\partial t = \nabla \times (\bar{v} \times \bar{B})$: in fact means $\bar{B}$ moves with $\bar{v}$ – we say $\bar{B}$ is FROZEN-IN to plasma flow, $\bar{v}$ (applies in most of interplanetary space, magnetosphere + F-region ionosphere)
- If L small, so $R_m << 1$, $\partial \bar{B}/\partial t = \nabla^2 \bar{B}/\mu_0 \sigma$ and field DIFFUSES through plasma. Actually, high σ ensures that this only occurs in highly localised (small L) regions

MAGNETIC RECONNECTION (Dungey, 1953; 1961)

– a breakdown of ideal MHD and 'frozen-in flux'

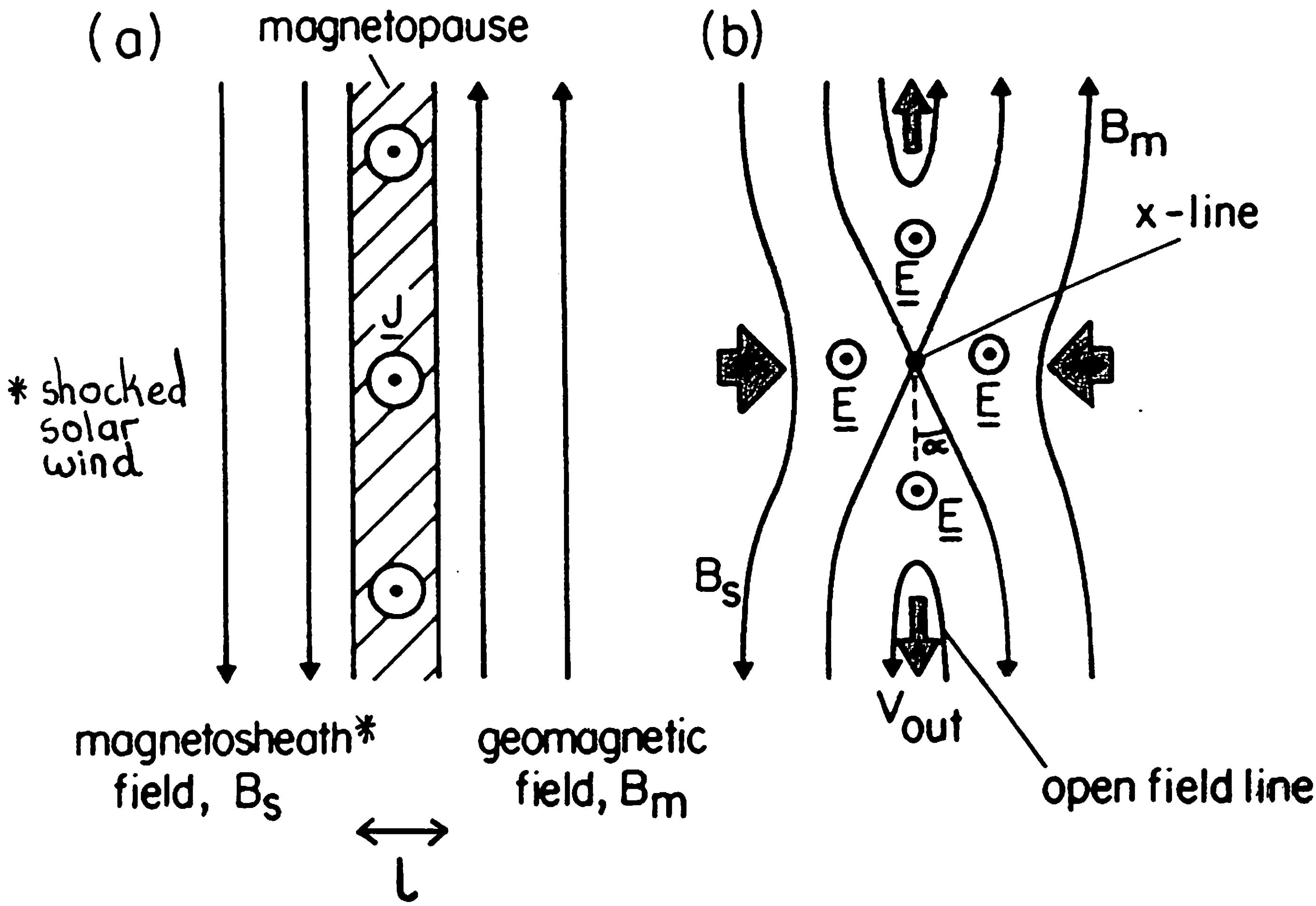

For ideal MHD, B_s and B_m cannot mix (both frozen-in)

If $\bar{B}_s \neq \bar{B}_m$ current must flow in magnetopause

Solar wind compresses current layer so $\boxed{L \text{ small}}$ and $\boxed{R_m \to 1}$. Hence diffusion of B through plasma becomes important.

Motion of $\bar{B}_s$ and $\bar{B}_m$ into X-line and of open field lines away from X-line, corresponds to an electric field, $\bar{E}$, along X-line, called the $\boxed{\text{reconnection rate}}$

Field Line Convection due to Magnetic Reconnection

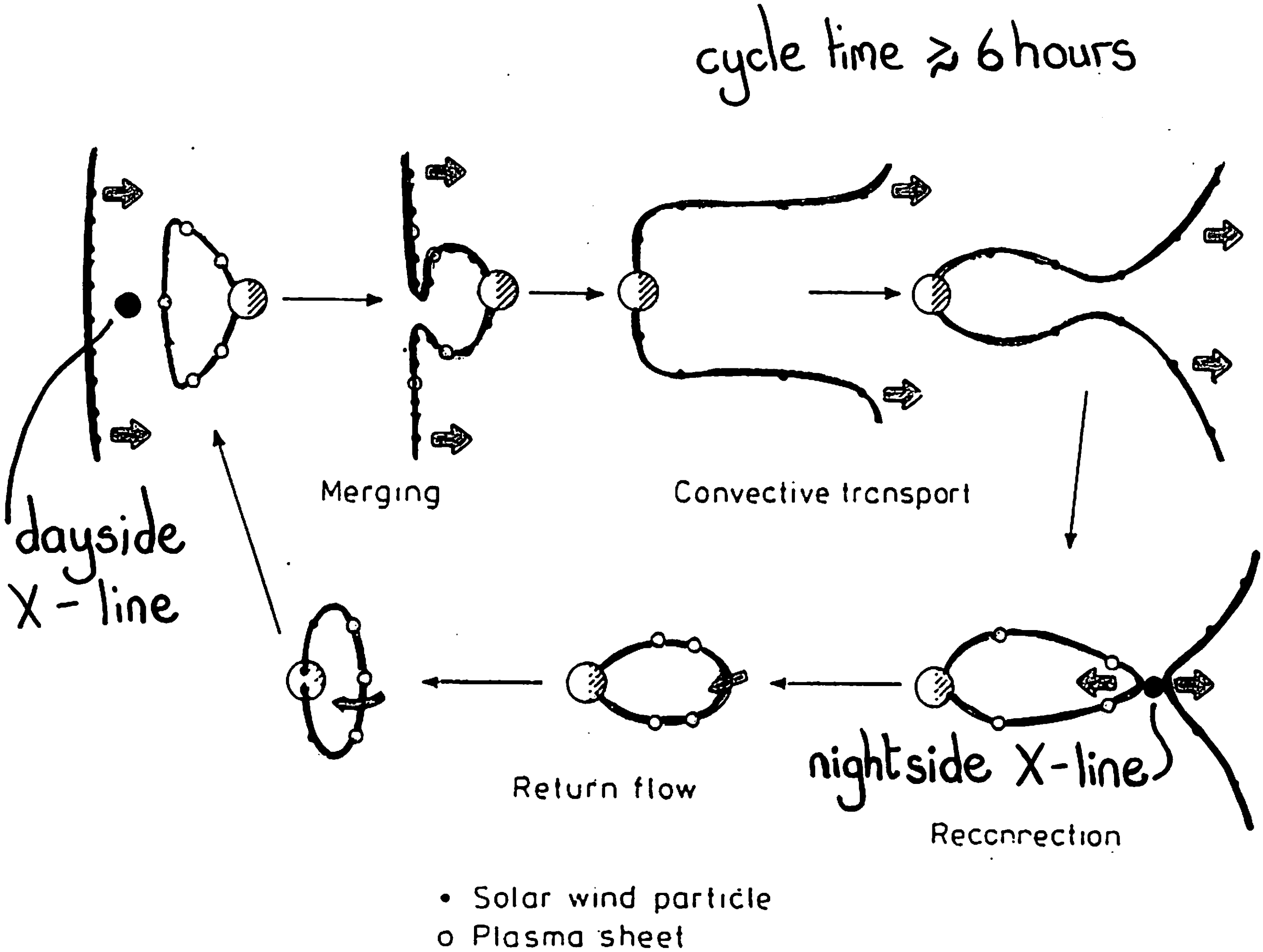

Figure 8.27 The history of a field line. (After S.-I. Akasofu, *Chapman Memorial Lecture*, 1973.)

— Interplanetary Field Line ($B_z < 0$)

— Closed Geomagnetic Field Line

— Open Field Line

Pedersen currents very important because:

- They close magnetospheric current systems
- Allow momentum transfer from the solar wind into the ionospher
- Deposit solar wind energy in the upper atmosphere

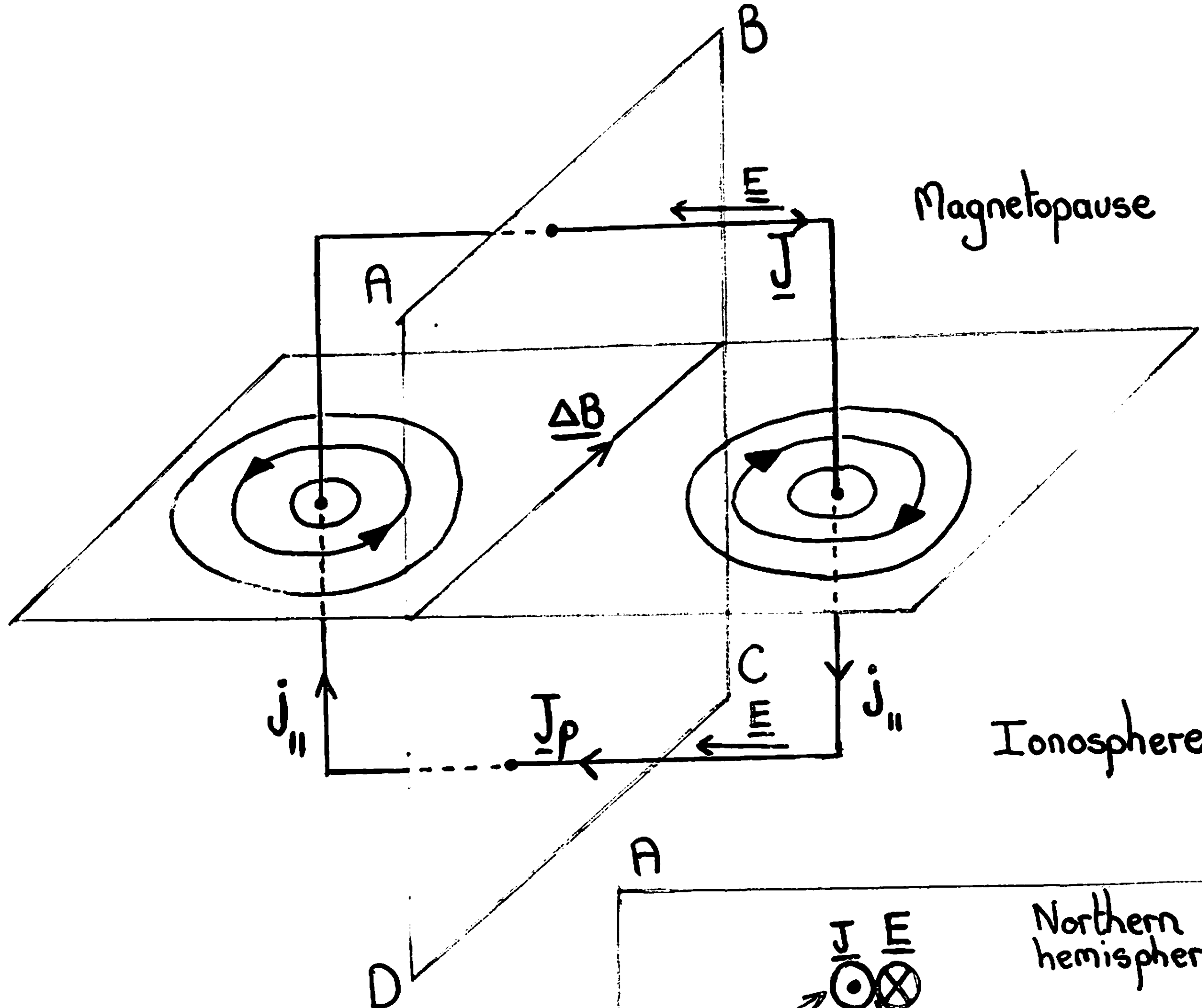

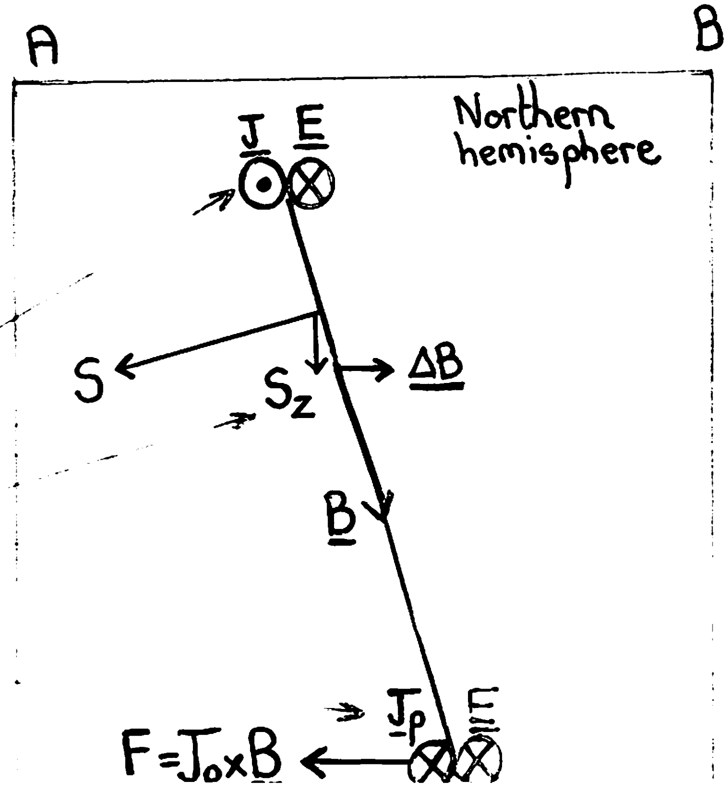

At magnetopause, $\underline{J} \cdot \underline{E} < 0$
(energy extracted from plasma)

At mid-altitudes, downward Poynting Flux, S_z

In ionosphere, $\underline{J} \cdot \underline{E} > 0$
(energy deposited in plasma)

A-2 MODEL

(IMF By < 0 for Northern hemisphere)

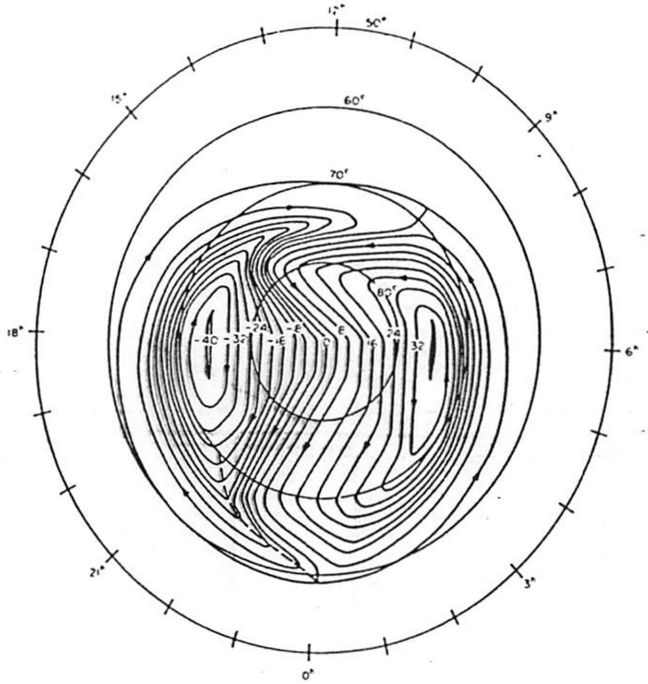

FIG. 7(a)

B-2 MODEL

(IMF By < 0 for southern hemisphere)

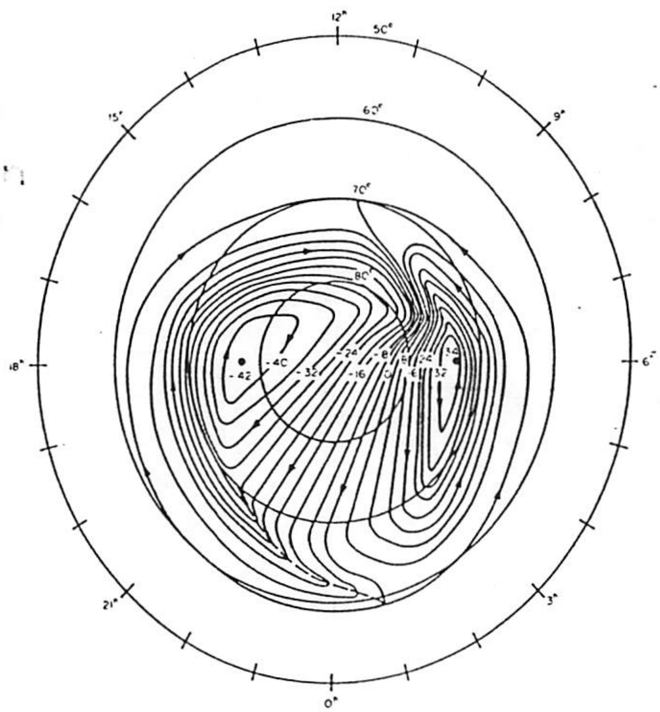

(b)

FIG. 7. POLAR CONVECTION ELECTRIC POTENTIAL DISTRIBUTIONS FROM HEPPNER (1983), WITH DEPENDENCE ON THE "Y" COMPONENT OF THE IMF.
(a) The A-2 field – applied to the Northern Hemisphere with BY – ve. Applied to the Southern Hemisphere with BY + ve.
(b) The B-2 field – applied to the Southern Hemisphere with BY – ve. Applied to the Northern Hemisphere with BY + ve.

. HEPPNER MODEL OF CONVECTION ELECTRIC POTENTIAL

Origins of magnetospheric and ionospheric convection

• 1. Reconnection

Transfer of open flux from dayside to nightside by solar wind

Return flow of closed field lines

• 2. Viscous-like interactions

any process which acts on closed field lines

"anything but reconnection"

includes:

"impulsive penetration"; wave-driven diffusion; gradient drift entry; Kelvin-Helmholtz waves; solar wind dynamic pressure changes; etc.

<u>BUT</u> how much of the apparently viscous effect is due to continuing tail reconnection of residual lobe open flux

Cowley, 1984

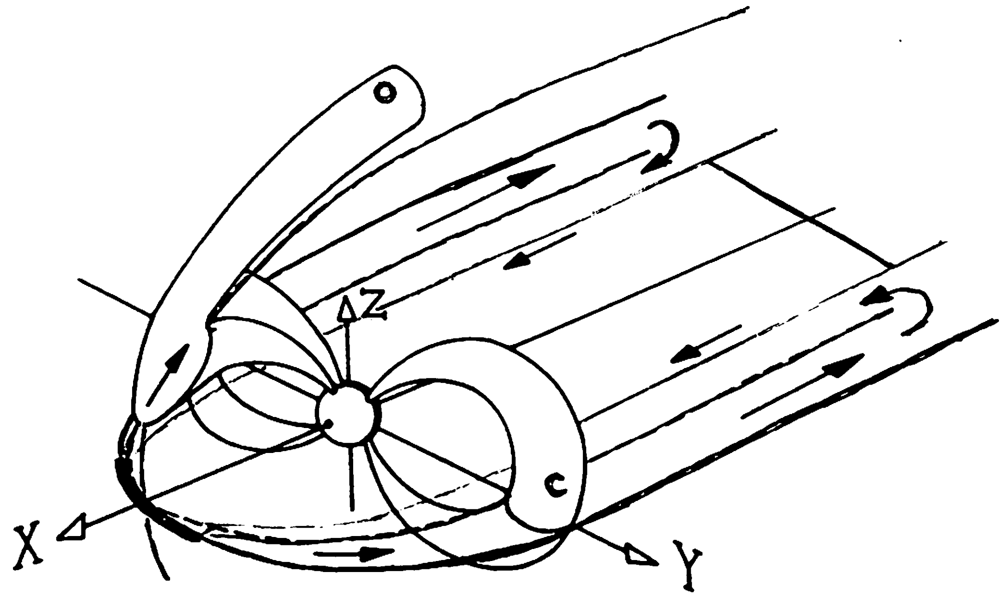

(a)

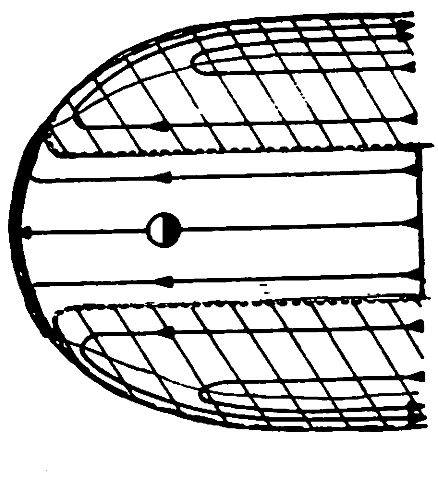

(b)

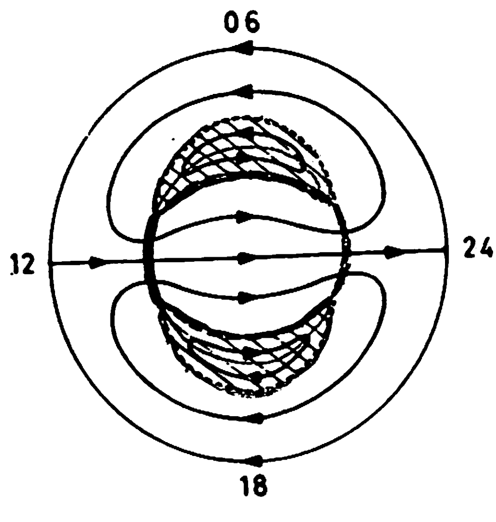

(c)

Satellite Flow Data

(Coley et al., 1987)

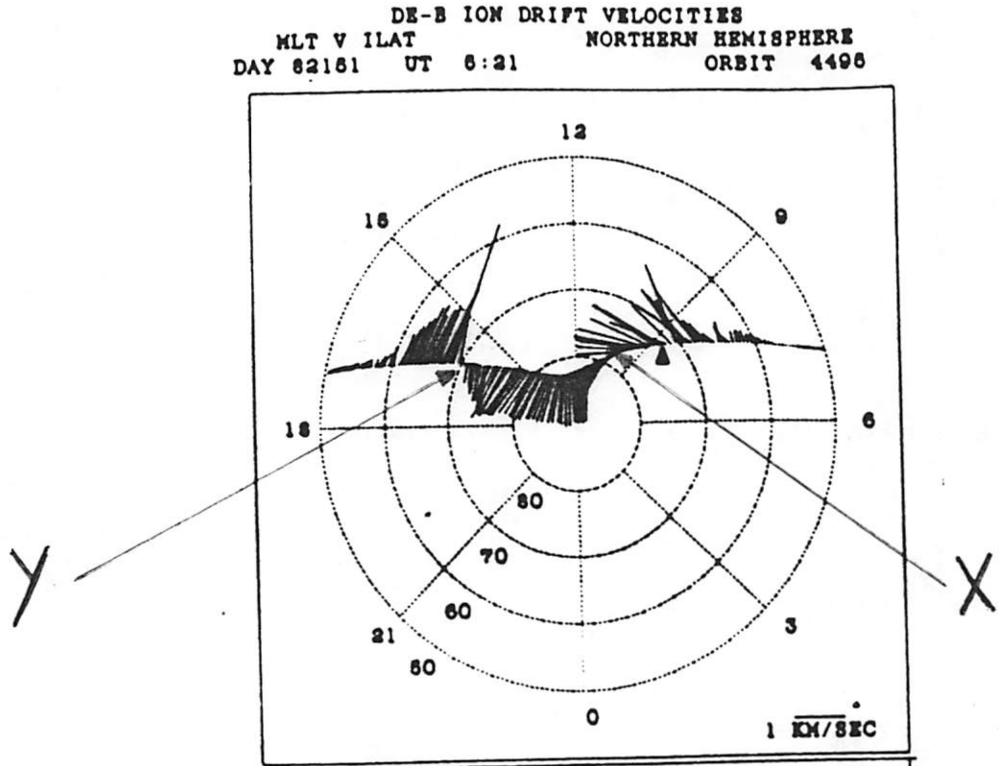

$$\phi_x = \int_{-\infty}^{x} E_{\perp}\, dl$$

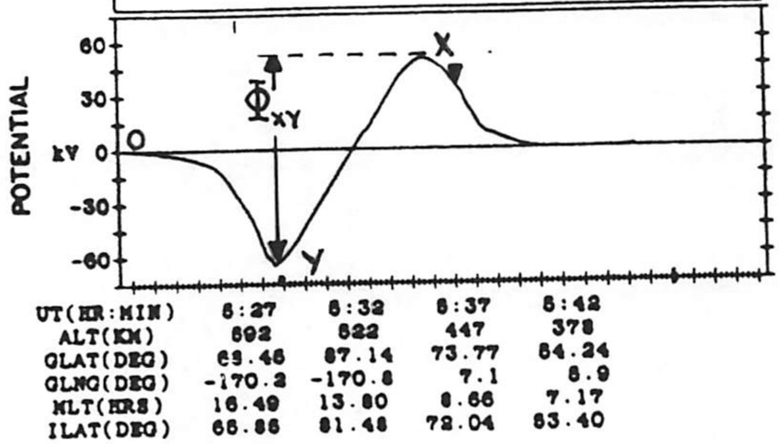

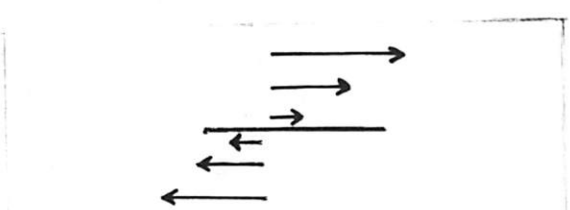

Shear reversal at Y

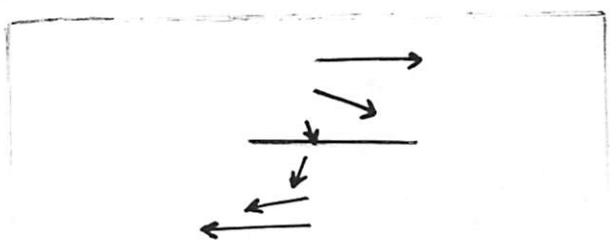

Rotational reversal at X

If X is near dawn and Y near dusk, Φ_{XY} is called the transpolar voltage, Φ

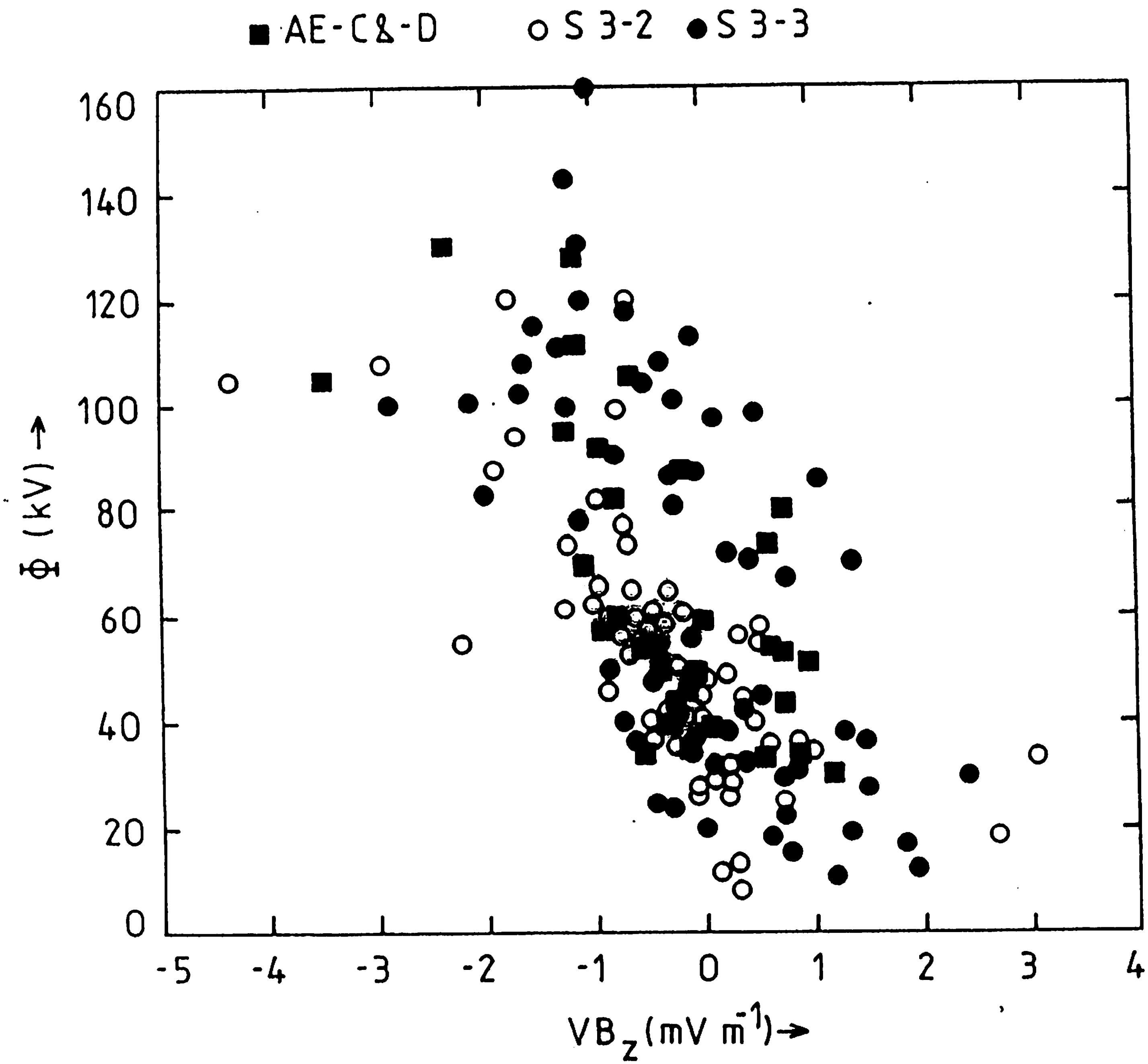

Reiff et al. (1981)
Doyle and Burke (198
Wygant et al. (1983)
Cowley (1984)

PLASMA FLOWS IN THE EQUATORIAL MAGNETOSPHERE

ELECTRIC EQUIPOTENTIALS OR FLOW LINES

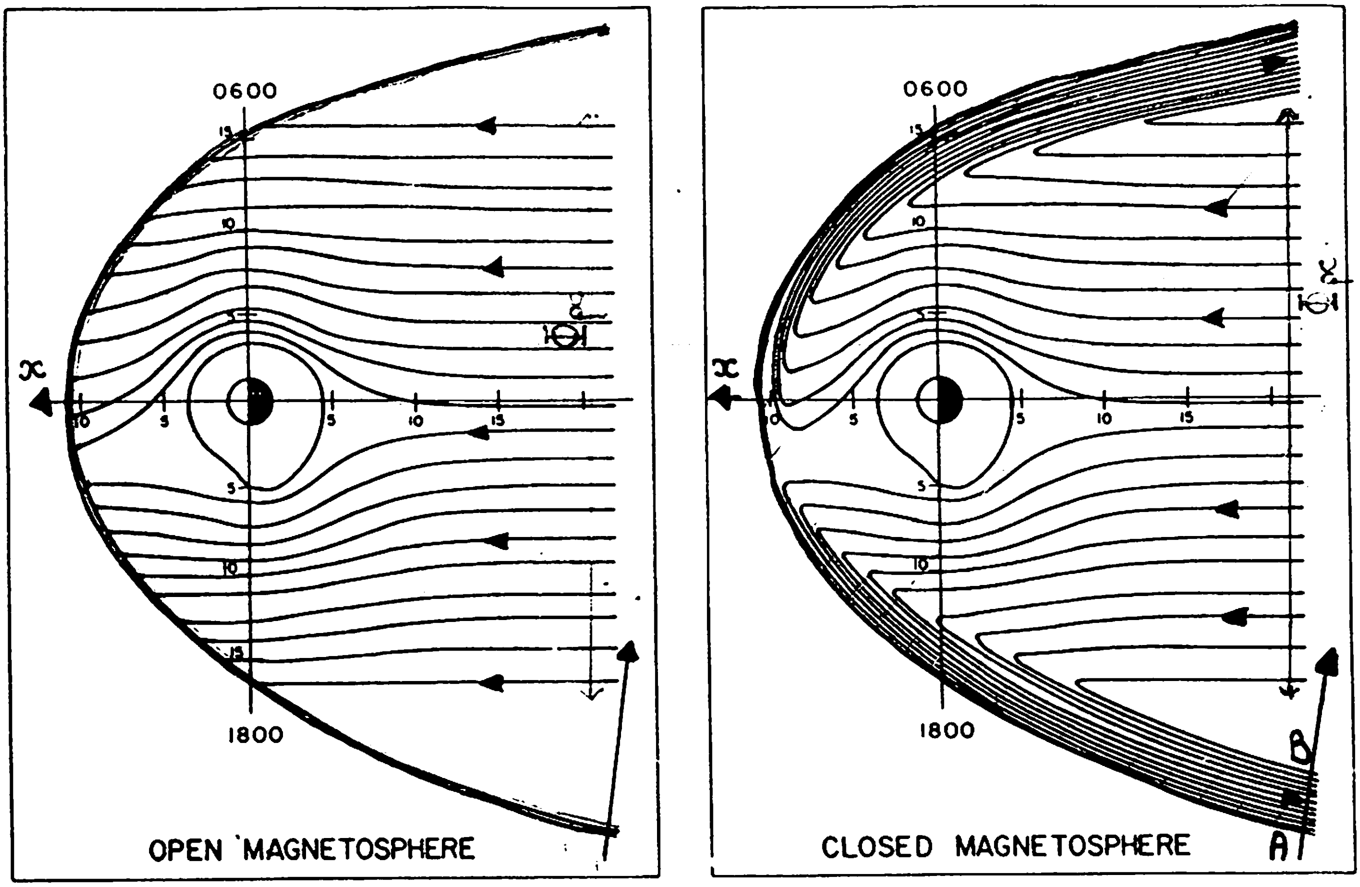

Fig. 1. Electric equipotentials (or E × B flow lines) in the equatorial plane of idealized completely open and completely closed magnetospheres.

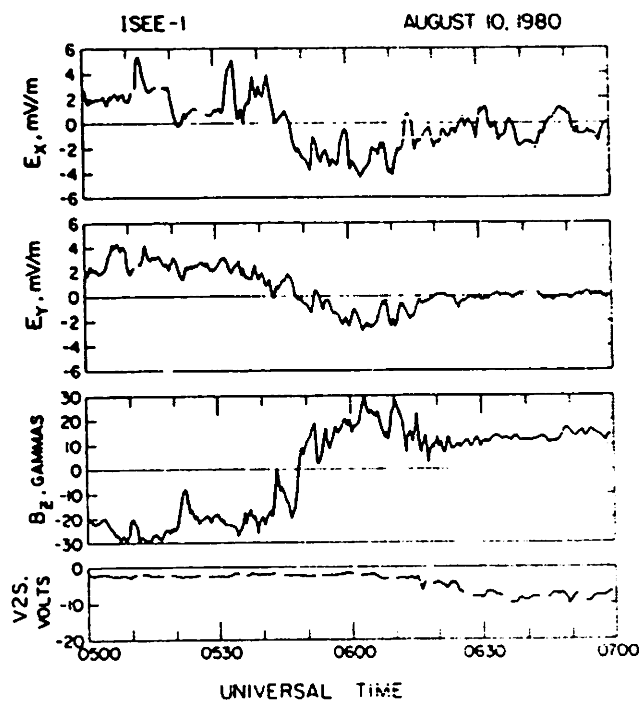

Fig. 2. Electric and magnetic fields measured before and after a dusk magnetopause crossing.

Consider electric field observations by a satellite moving into magnetosphere at low magnetic latitudes, as shown

Plasma drift, $\bar{v} = \bar{E} \times \bar{B} / B^2$

$\therefore$ drift normal to path $\equiv$ electric field component along path, E_o

voltage, $\Phi_v = \int_A^B E_o \, dl$

where A and B are the edges of the anti-sunward moving LLBL

For fully-open magnetosphere $\Phi_v = 0$

Mozer, Geophys. Res. Lett., 11, 135, 1984

[NB. In comment, Heikkila (Geophys. Res. Lett., 9, 877, 1986) claims LLBL was not crossed far enough down tail to see full Φ_V].

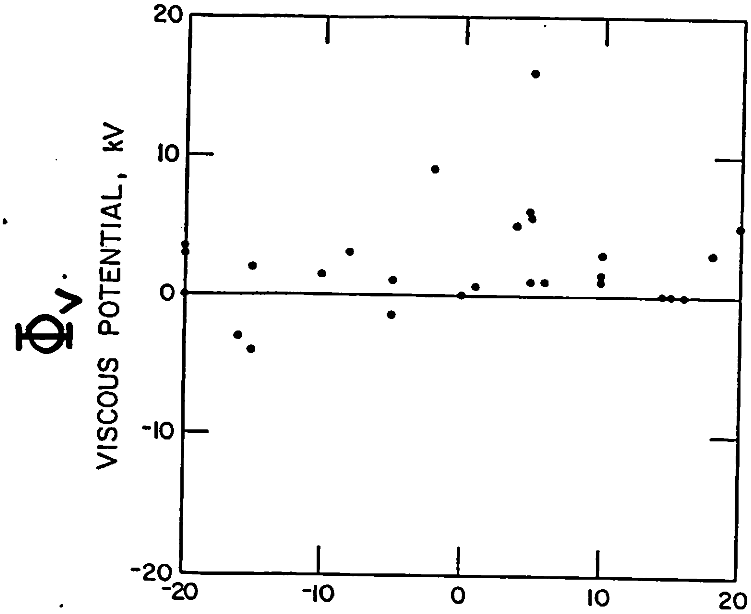

Fig. 4. Scatter plot of the viscous interaction potential versus B_z for 28 magnetopause crossings within 2 hours of local dusk.

Φ_V is less than 15 kV in all cases and typically < 5 kV.

If Φ_V is the same on both flanks

total contribution to Φ_{pc} of viscous-like interactions is typically 10 kV and less than 30 kV in all cases (consistent with Φ_{pc} observed during northward IMF)

We Conclude: Reconnection contributes up to ~100 kV to Φ_{pc}
Viscous-like interaction contribute $\lesssim$ 20 kV

Svalgaard - Mansurov Effect

as explained by
Jörgensen et al. (1972)
Atkinson (1972)
Cowley (1981)

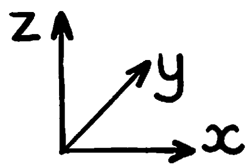

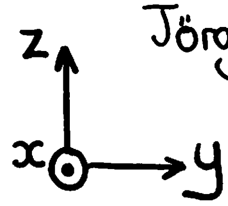

IMF $B_y > 0$

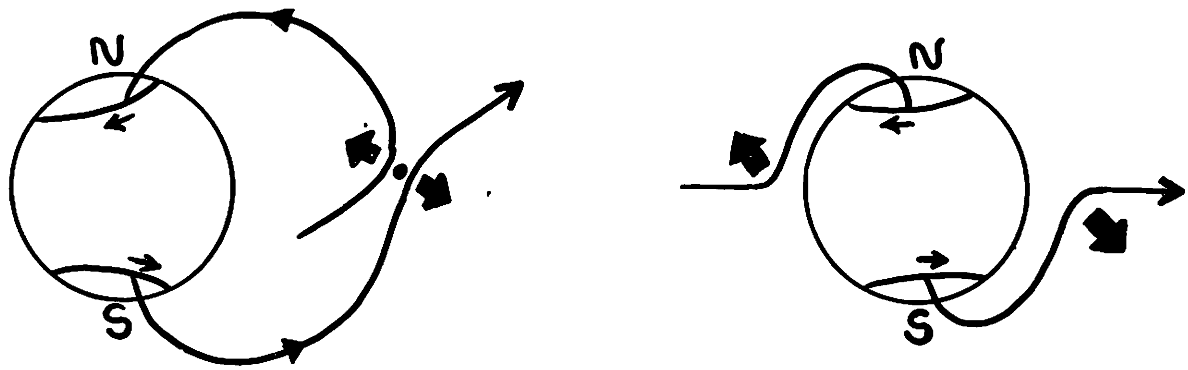

Westward } flow in { Northern } hemisphere
Eastward } flow in { Southern } hemisphere

IMF $B_y < 0$

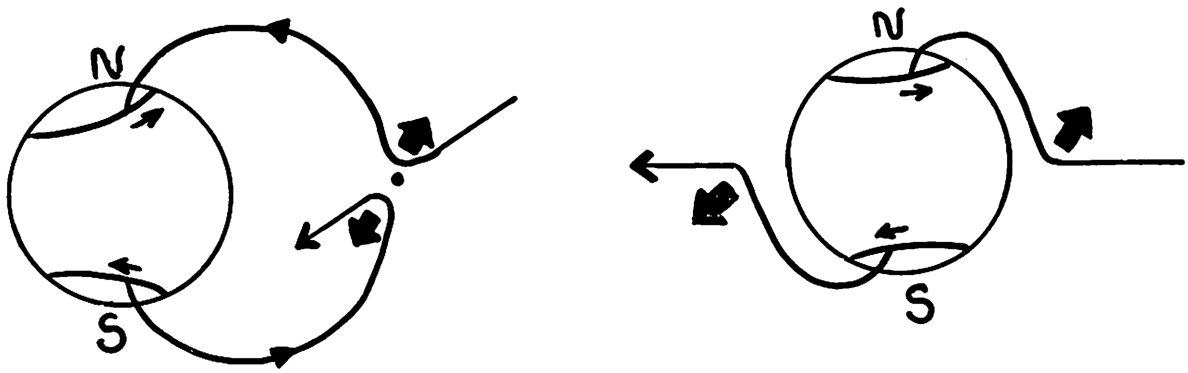

Eastward } flow in { Northern } hemisphere
Westward } flow in { Southern } hemisphere

A. $B_y > 0$

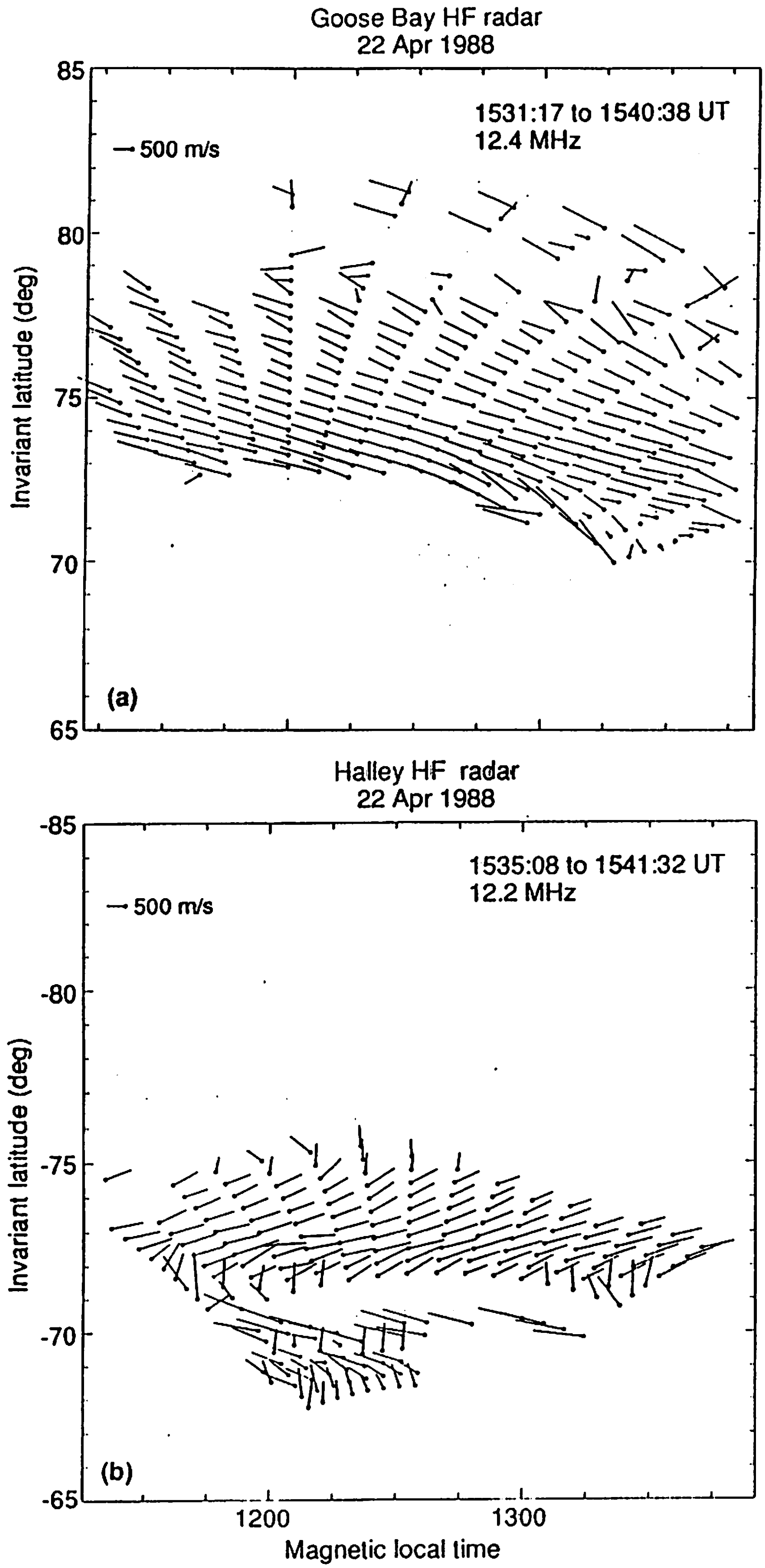
Goose Bay HF radar
22 Apr 1988
1531:17 to 1540:38 UT
12.4 MHz
500 m/s
Invariant latitude (deg)
85
80
75
70
65
(a)
Halley HF radar
22 Apr 1988
1535:08 to 1541:32 UT
12.2 MHz
500 m/s
Invariant latitude (deg)
-85
-80
-75
-70
-65
(b)
1200
1300
Magnetic local time

Fig. 6

B. $B_y < 0$

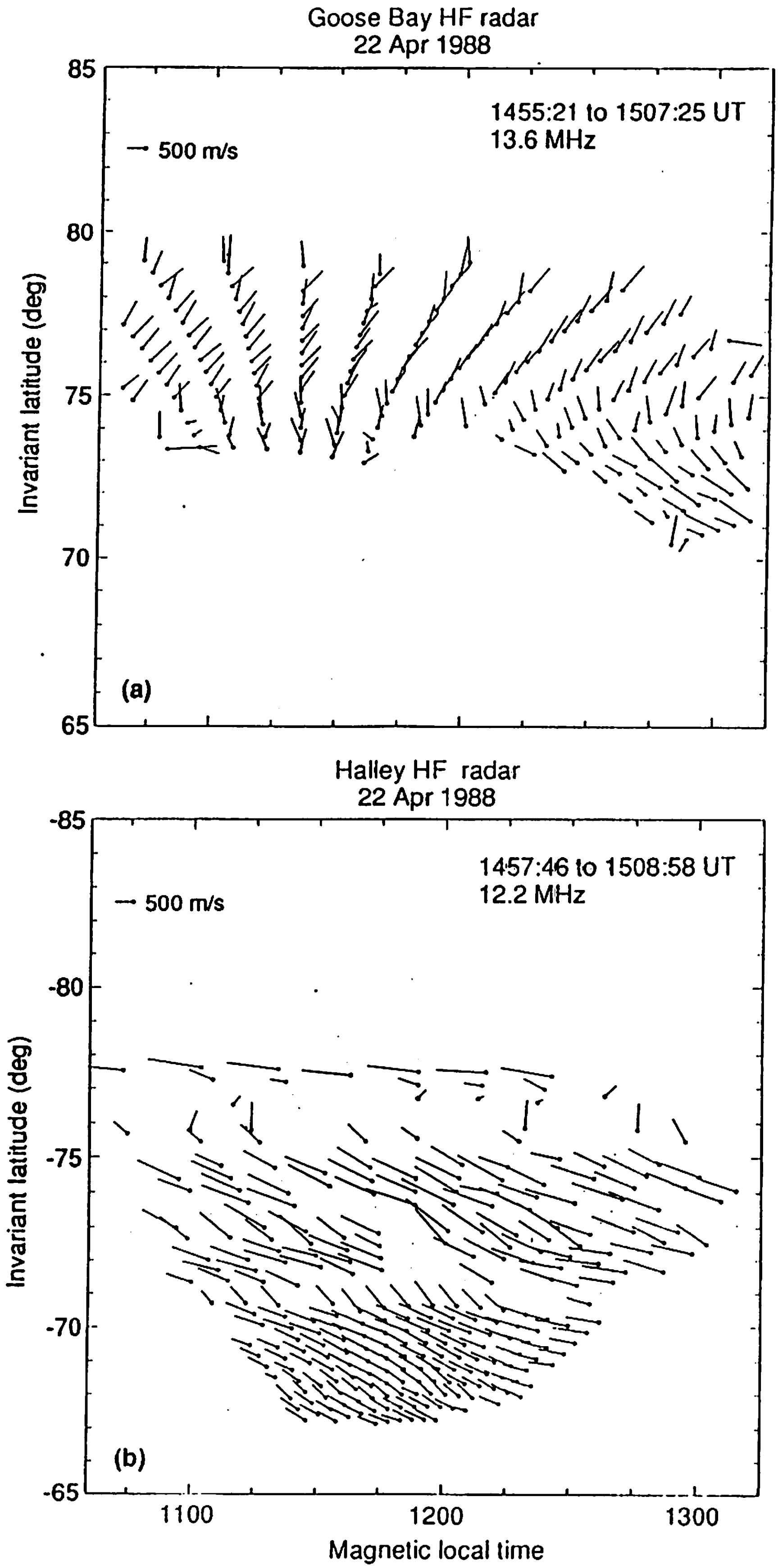
Goose Bay HF radar
22 Apr 1988
1455:21 to 1507:25 UT
13.6 MHz
500 m/s
Invariant latitude (deg)
85
80
75
70
65
(a)
Halley HF radar
22 Apr 1988
1457:46 to 1508:58 UT
12.2 MHz
500 m/s
Invariant latitude (deg)
-85
-80
-75
-70
-65
(b)
1100
1200
1300
Magnetic local time

Fig. 7

THE JOHNS HOPKINS UNIVERSITY
APPLIED PHYSICS LABORATORY
LAUREL MARYLAND

event C
N. hemisphere
+ → −

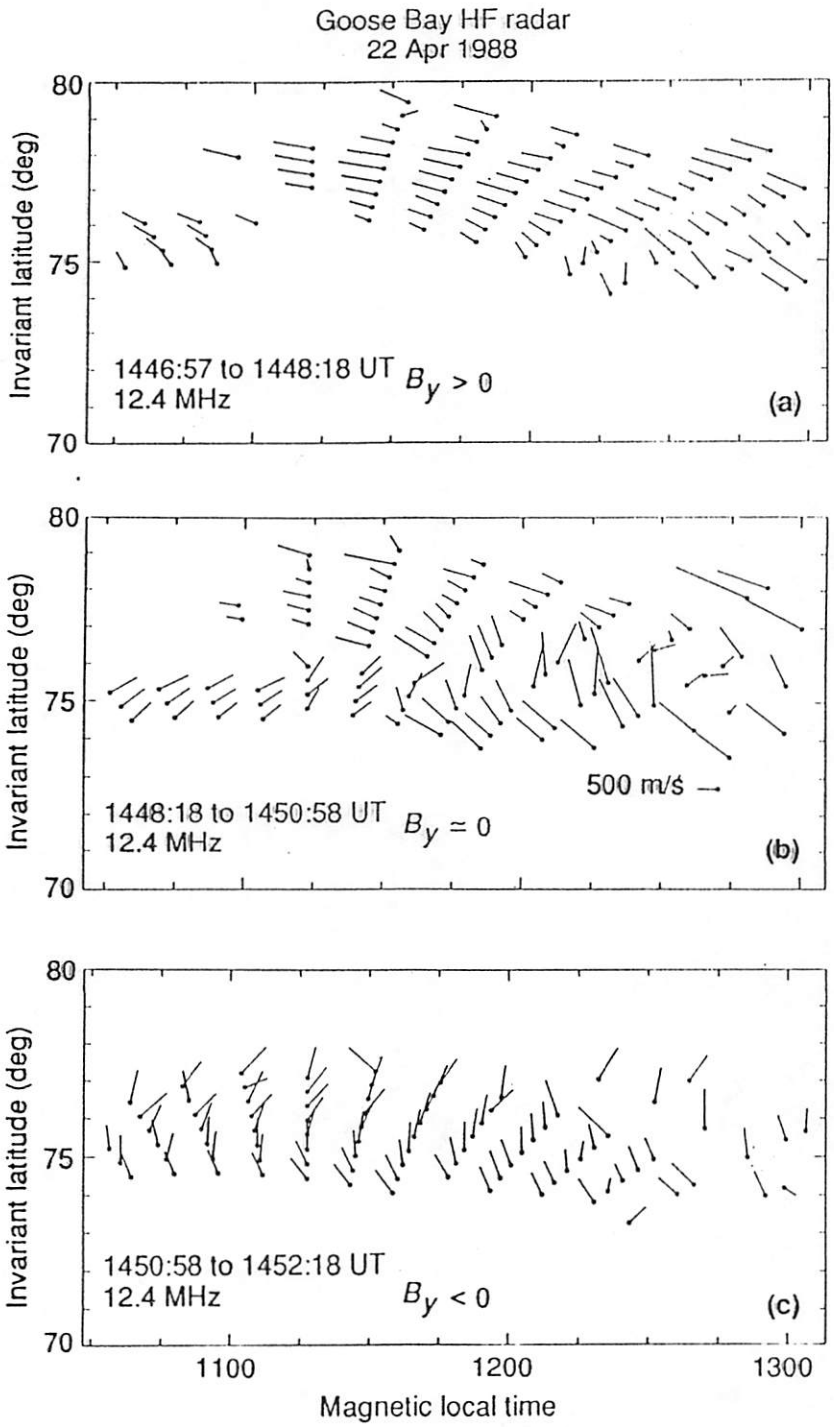

Fig. 9

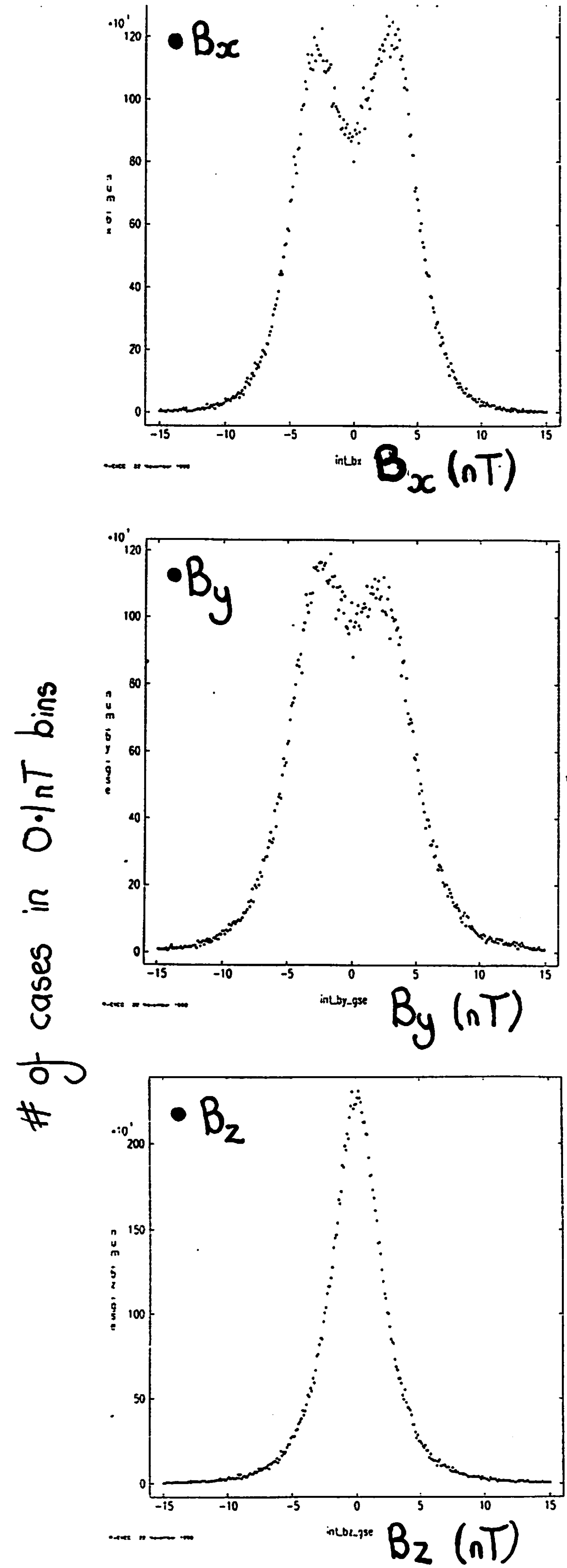

24 years' IMF data (hourly averages)

CONVECTION FOR NORTHWARD IMF

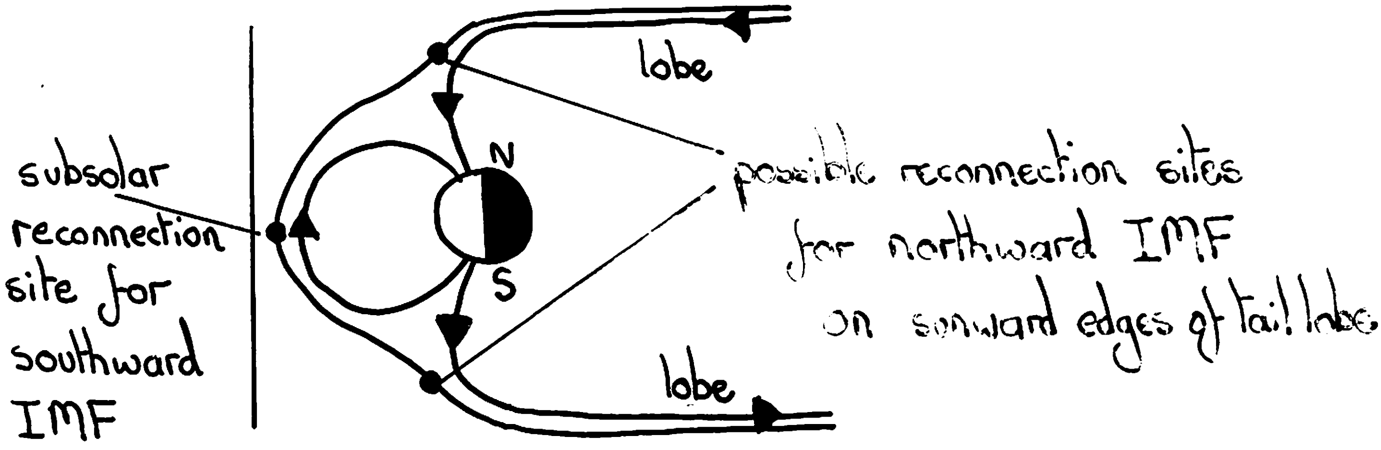

Introduces "lobe cells" into polar cap convection
(NB. I assume open lobes never disappear completely)

If reconnection occurs at one or other lobe, possibly depending on IMF B_x (?) (Northern hemisphere favoured for $B_x < 0$?)

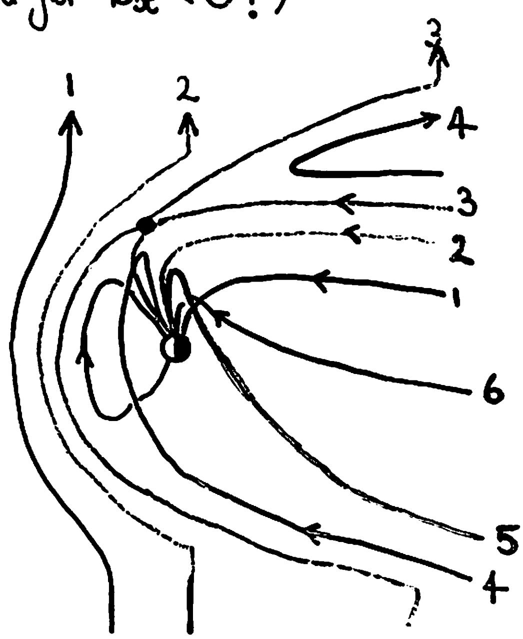

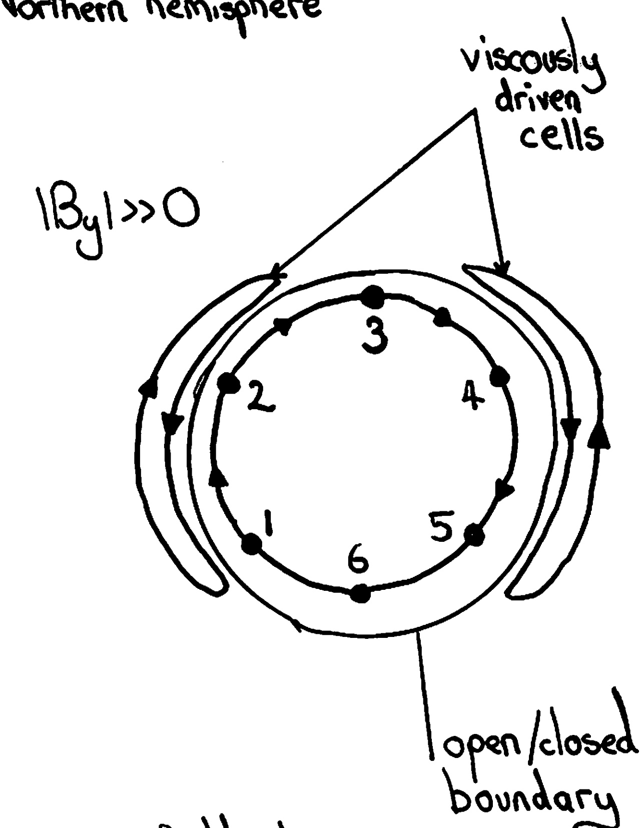

This "stirring" effect re-configures open field lines and causes circulation on open field lines.

Inferred convection patterns in the Northern hemisphere

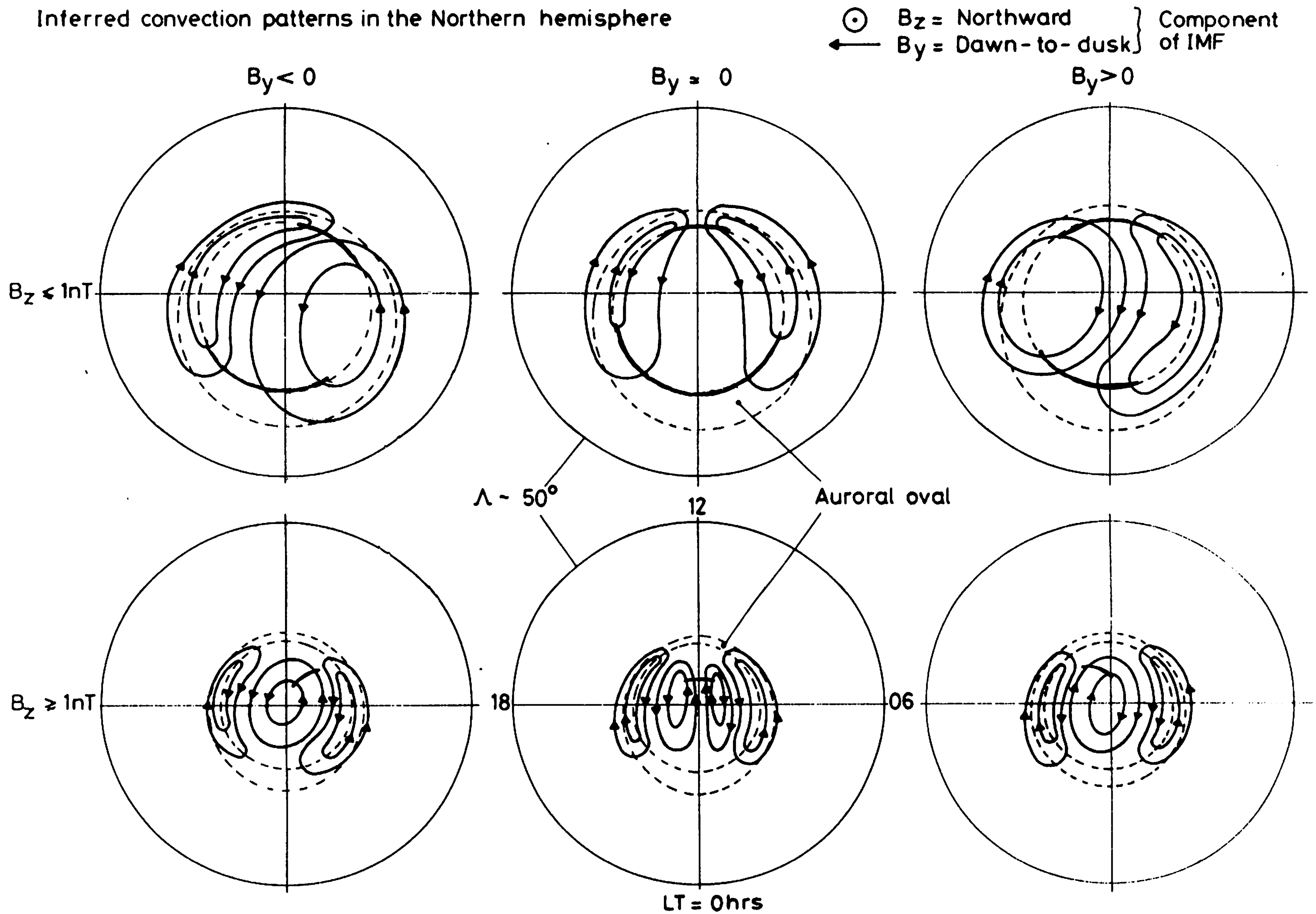

All steady-state patterns because no account taken of IMF or magnetospheric history

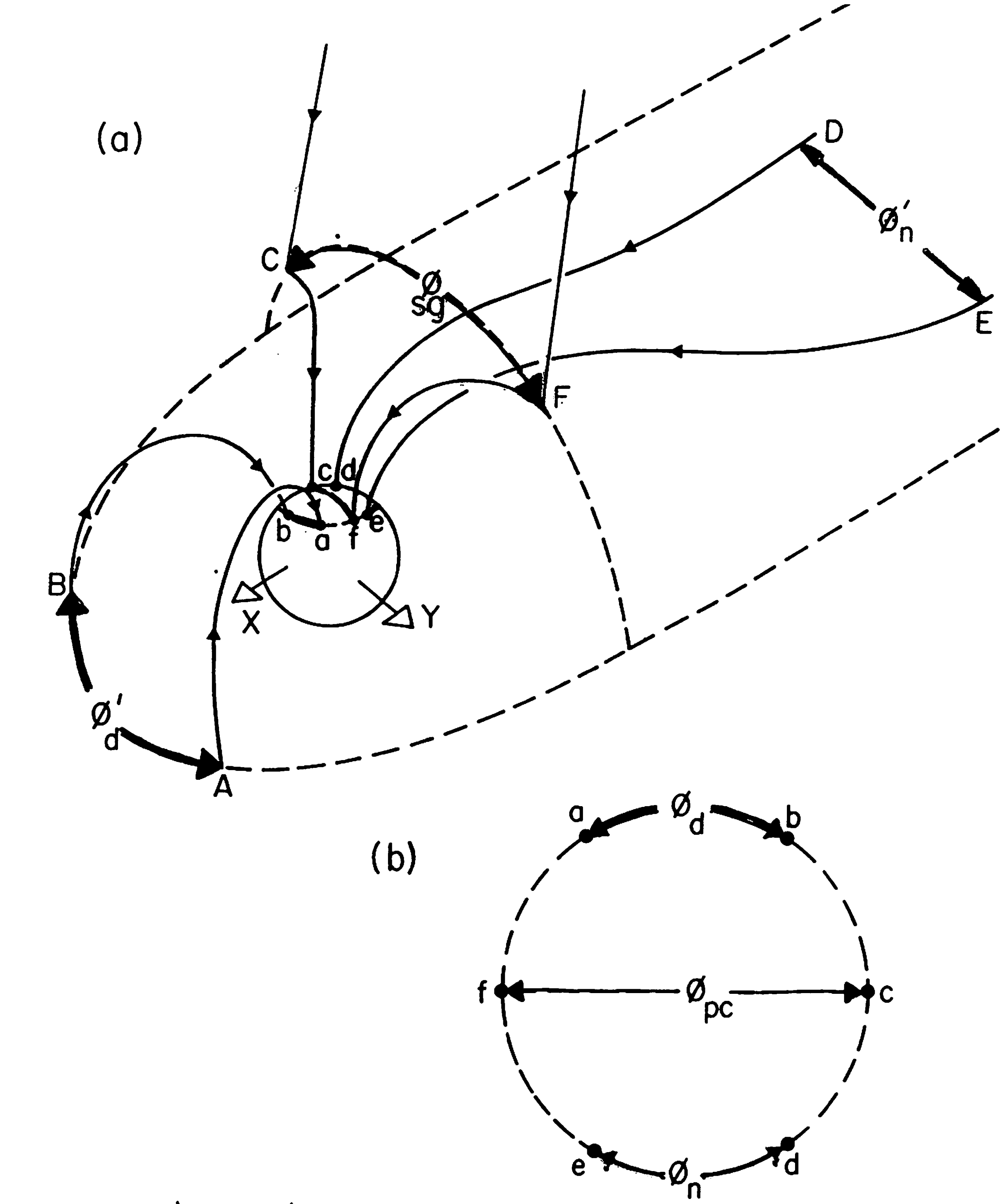

Only in steady-state:

$$\phi_{pc} = \phi_{sg} = \phi_d = \phi_d' = \phi_n = \phi_n'$$

Generally, apply Faraday's Law, e.g. to cCFf

$$\phi_{pc} - \phi_{sg} = \frac{d}{dt} \int_{cCFf} \bar{B} . d\bar{A} \neq 0 \qquad (E_{\parallel} \text{ negligible})$$

Polar Cap Expansion / Contraction

shows steady state does not always (indeed often) apply

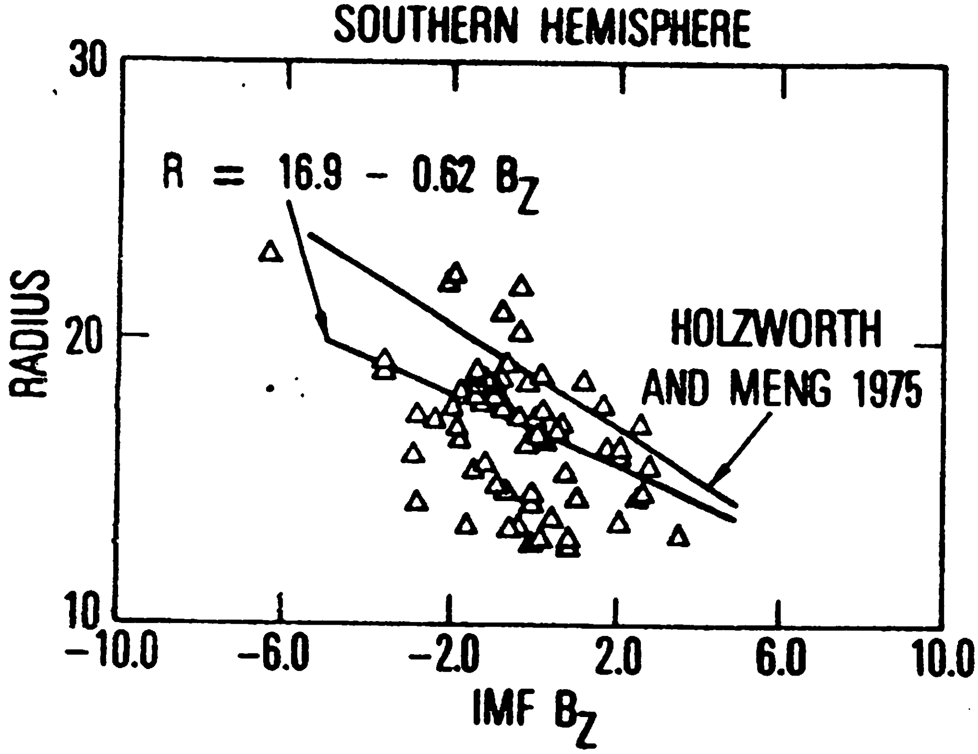

FIG. 3. COMPARISON OF CIRCLE RADIUS *R* FROM THIS STUDY AND PREVIOUS STUDY.

Polar Cap Flux, $F = B_i \pi R^2$

$$R = 16{\cdot}9 - 0{\cdot}62 B_z \quad \text{(deg.)}$$

gives $F = (571{\cdot}2 - 46 B_z + 0{\cdot}76 B_z^2) \times 10^6$ Wb

(B_z in nT)

$B_z = +5\text{nT}$, $F \approx 3{\cdot}6 \times 10^8$ Wb

$B_z = -5\text{nT}$, $F \approx 8{\cdot}2 \times 10^8$ Wb

$\Delta F/\Delta t \sim 130\text{kV} = |\phi_d - \phi_n|$ (for $\Delta t = 1$ hr.)

Effect of propagation delay between dayside and nightside X-line ($\gtrsim 30$ min.) :-

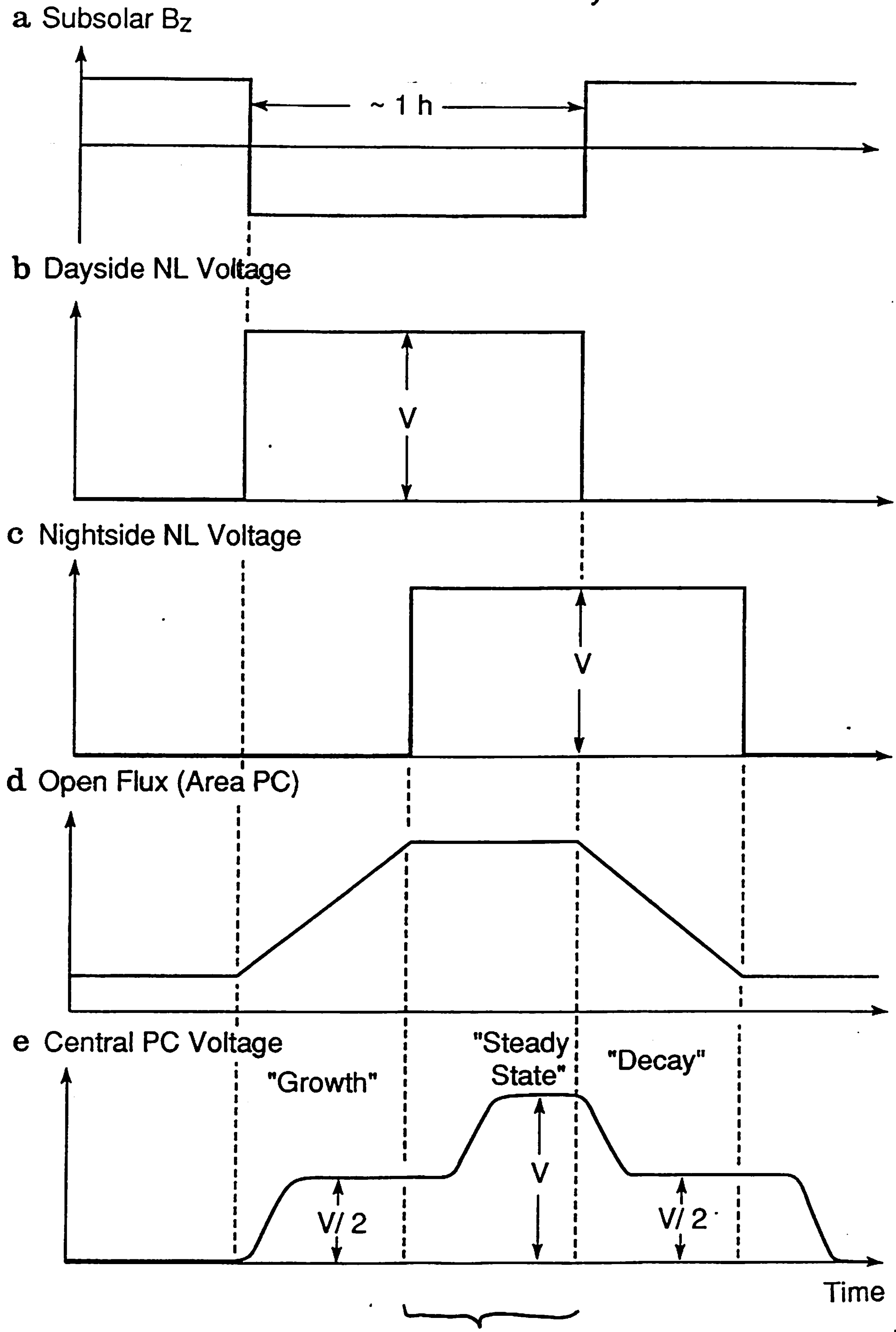

in fact unlikely that $\phi_d' = \phi_n'$, even after ϕ_n' has responded $\therefore$ this steady state unlikely

Stability of Polarity of IMF B_z

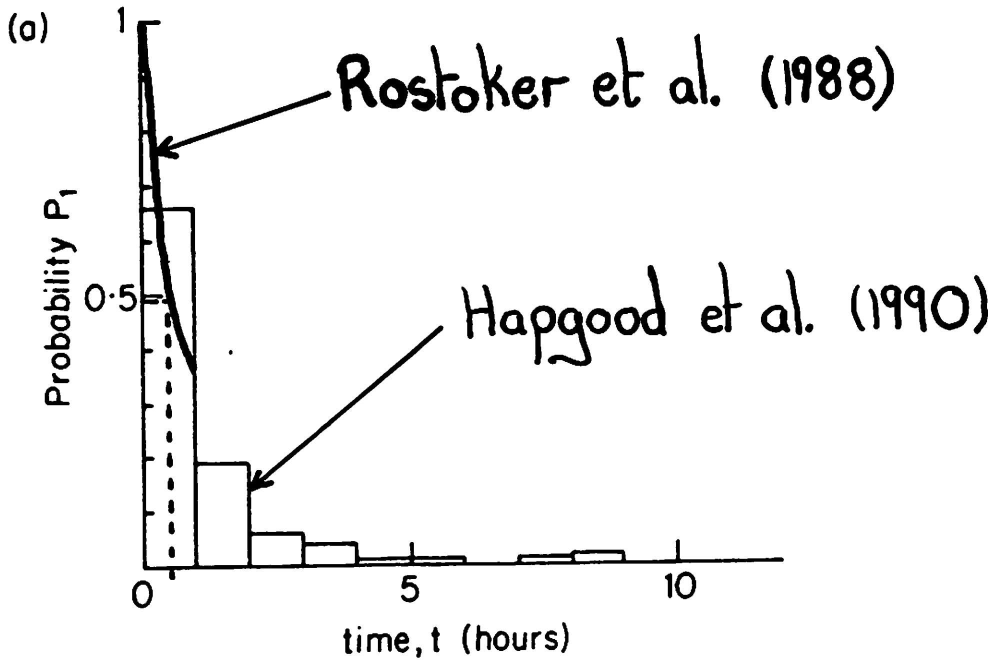

P_1 is the probability that the IMF B_z component remains constant for a time t

$P_1 \approx 0.5$ for $t = 30$min.

Cowley and Lockwood point out that information about ϕ_d' cannot reach DE for $t^* \gtrsim 30$min. Probability that ϕ_d' has changed polarity by then, $P_1^* \gtrsim 0.5$

Hence even if $\phi_n'(t^*) = \phi_d'(0)$ as soon as information reaches DE, $\phi_n'(t^*) \neq \phi_d'(t^*)$ i.e. NOT STEADY STATE

Electric field mapping

FLUX TUBE from magnetopause (m) to ionosphere (i)

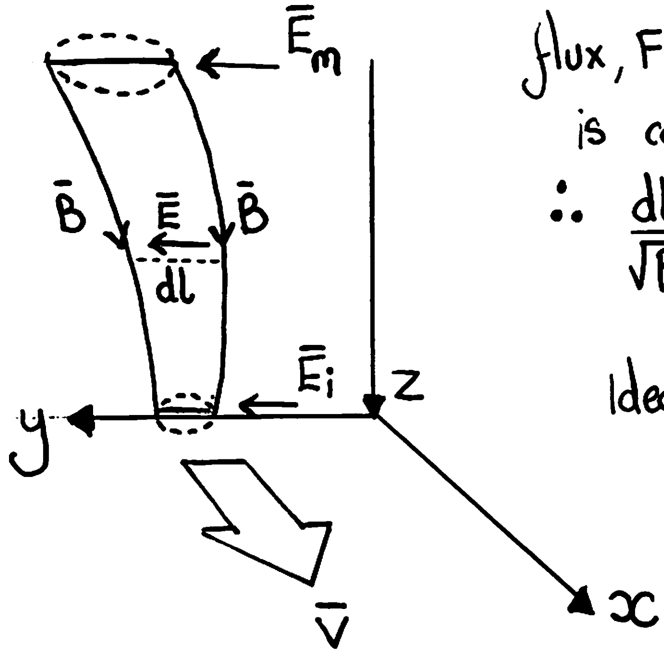

flux, $F = B.\pi dl^2/4$ is constant

$\therefore \dfrac{dl}{\sqrt{B}}$ is constant w.r.t. s (distance along flux tube)

Ideal MHD so $E_{\parallel} = 0$

Faraday's Law yields:

$$\oint \bar{E}.\bar{dl} = E_m dl_m - E_i dl_i = \int_i^m \frac{\partial B_x}{\partial t}.dl.ds$$

$$\boxed{\frac{E_m}{\sqrt{B_m}} - \frac{E_i}{\sqrt{B_i}} = \int_i^m \left(\frac{\partial B_x}{\partial t}\right)\frac{1}{\sqrt{B}}\,ds}$$

In STEADY-STATE $(\partial B_x/\partial t) = 0$

($\therefore$ curl $\bar{E} = 0$, often called curl-free approximation)

$$\frac{E_m}{\sqrt{B_m}} = \frac{E_i}{\sqrt{B_i}}$$

Often used but only applies to steady-state limit.

Non-Steady Effects

and mapping the solar wind electric field down open field lines.

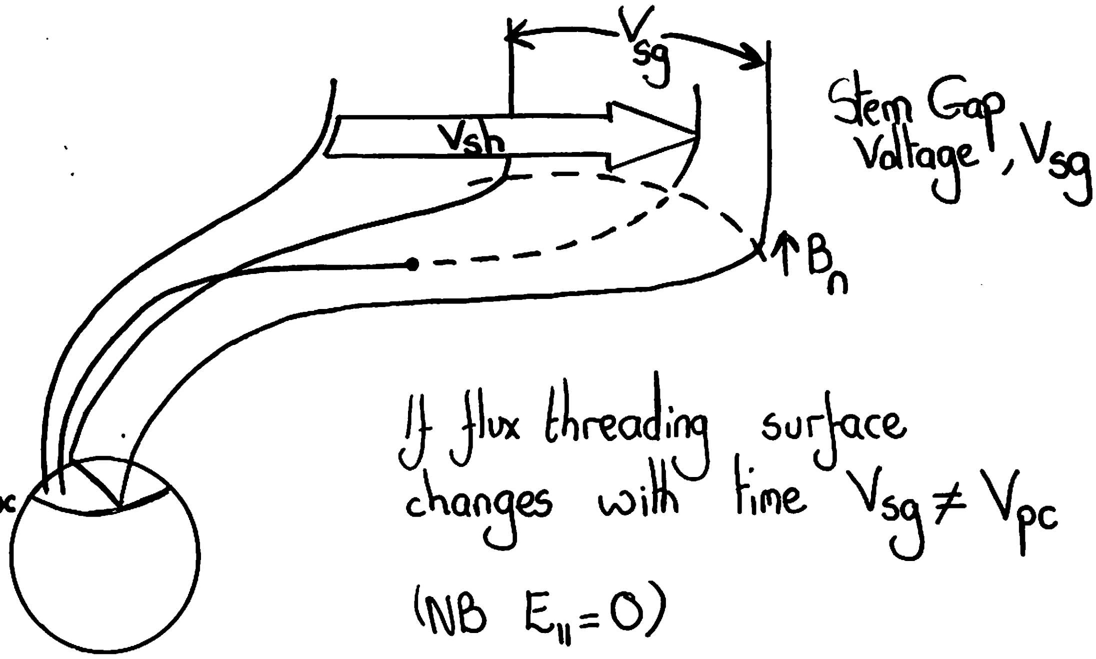

If flux threading surface changes with time $V_{sg} \neq V_{pc}$

(NB $E_{\parallel} = 0$)

If $V_{sh} = 450\ \text{kms}^{-1}$, $B_n = 5\text{nT}$ $\quad E_m = v_{sh} B_n = 2.25\ \text{mVm}^{-1}$

(For a Stern Gap width of $7 R_E$, $V_{sg} = 2.25 \times 10^{-3} \times 7 \times 6370 \times 10^3 \approx 100\text{kV}$)

[In steady-state

$$V_{sg} = V_{pc}$$

$$E_m / \sqrt{B_m} = E_i / \sqrt{B_i}$$

for $B_m \approx 50\text{nT}$; $B_i \approx 5 \times 10^{-5}\text{T}$

$E_i = 70\ \text{mV m}^{-1}$ $\qquad V_i = E_i / B_i \approx 1.4\ \text{km s}^{-1}$]

$$\frac{E_m}{\sqrt{B_m}} - \frac{E_i}{\sqrt{B_i}} = \int_i^m \left(\frac{\partial B_x}{\partial t}\right)\frac{1}{\sqrt{B}}\,ds$$

Let us consider $(\partial B_x/\partial t)$ needed to make $E_i = 0$ for this $E_m = 2.25\ \mathrm{mV\,m^{-1}}$ and $B_m = 50\,\mathrm{nT}$, by assuming $(\partial B_x/\partial t)$ is independent of s

Can then use a model field (Tsyganenko T87 model) to compute $\int_i^m \frac{1}{\sqrt{B}}\,ds$

For Stern Gap at $X = -15R_E$, $\int_i^m B^{-1/2} ds \approx 10^{12}\,\mathrm{m\,T^{-1/2}}$

$$E_i = 0 \quad \text{if} \quad \frac{\partial B_x}{\partial t} = \frac{2.25\times10^{-3}/(50\times10^{-9})^{1/2}}{10^{12}} = 10^{-11}\,\mathrm{T\,s^{-1}}$$

$$= 0.01\,\mathrm{nT\,s^{-1}}$$

Substorm growth phase typically lasts ~ 45 min $= 2700$ s.

during which $\Delta B_x \sim \left(\frac{\partial B_x}{\partial t}\right)\Delta t$
$\sim 27\,\mathrm{nT}$

Field changes of this magnitude are observed during substorm growth phases (eg. Fairfield and Ness, 1970; Fritz, 1984) <u>implying Stern Gap voltage of 100 kV need not cause any ionospheric flow,</u> throughout a growth phase lasting 45 min.

(instead, magnetic energy is stored in the tail)

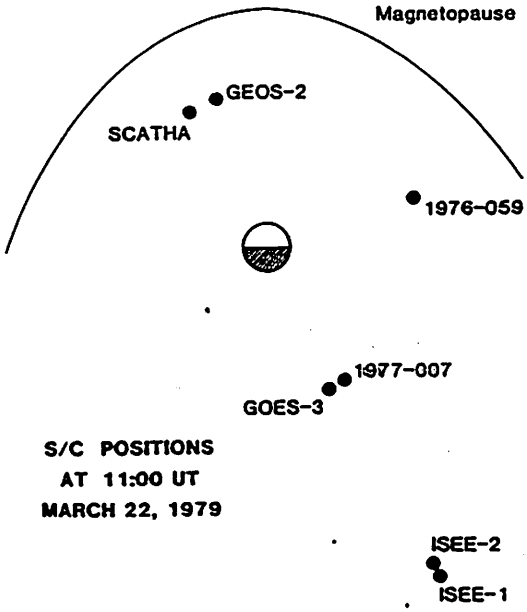

Figure 1. Location of seven spacecraft during the CDAW-6 substorm of 11 UT on March 22, 1979. Note the radial alignment of four satellites along the 0200 LT meridian with ISEE-1 at a GSE position of $(-13.6\ R_E, -7.2\ R_E, 0.6\ R_E)$ and ISEE-2 at $(-12.1\ R_E, -7.1\ R_E, 0.3\ R_E)$. The relative positions of these satellites changed very little during the event discussed here.

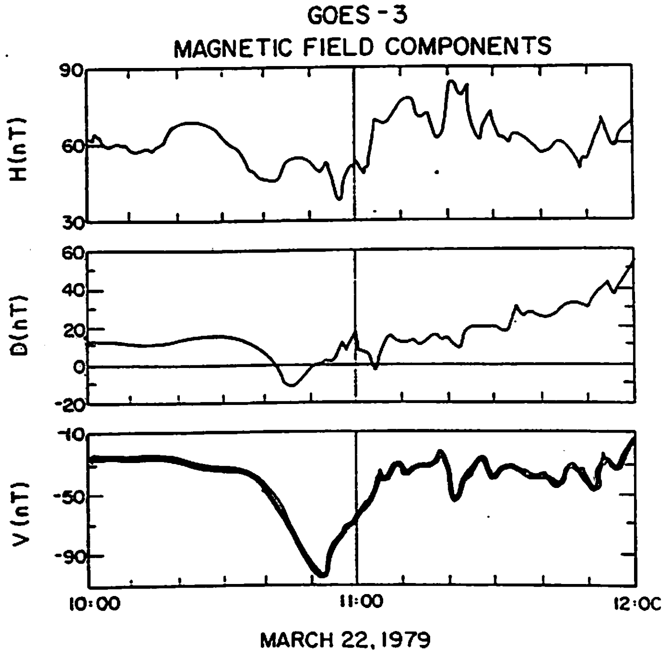

Figure 3. Magnetic field measurements made by the magnetometer on satelli GOES-3 during the CDAW-6 substorm of 11 UT on March 22, 1979. See te definition of V, D, and H components.

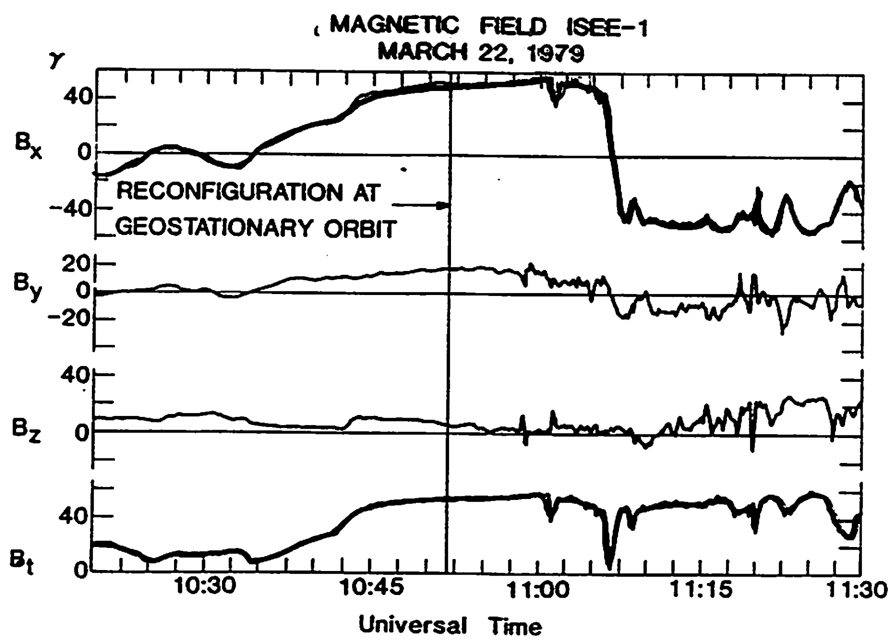

Figure 5. Magnetic field measurements in GSE coordinates made by the magnetometer on satellite ISEE-1 during the CDAW-6 substorm of 11 UT on March 22, 1979.

Fritz et al. (1984)

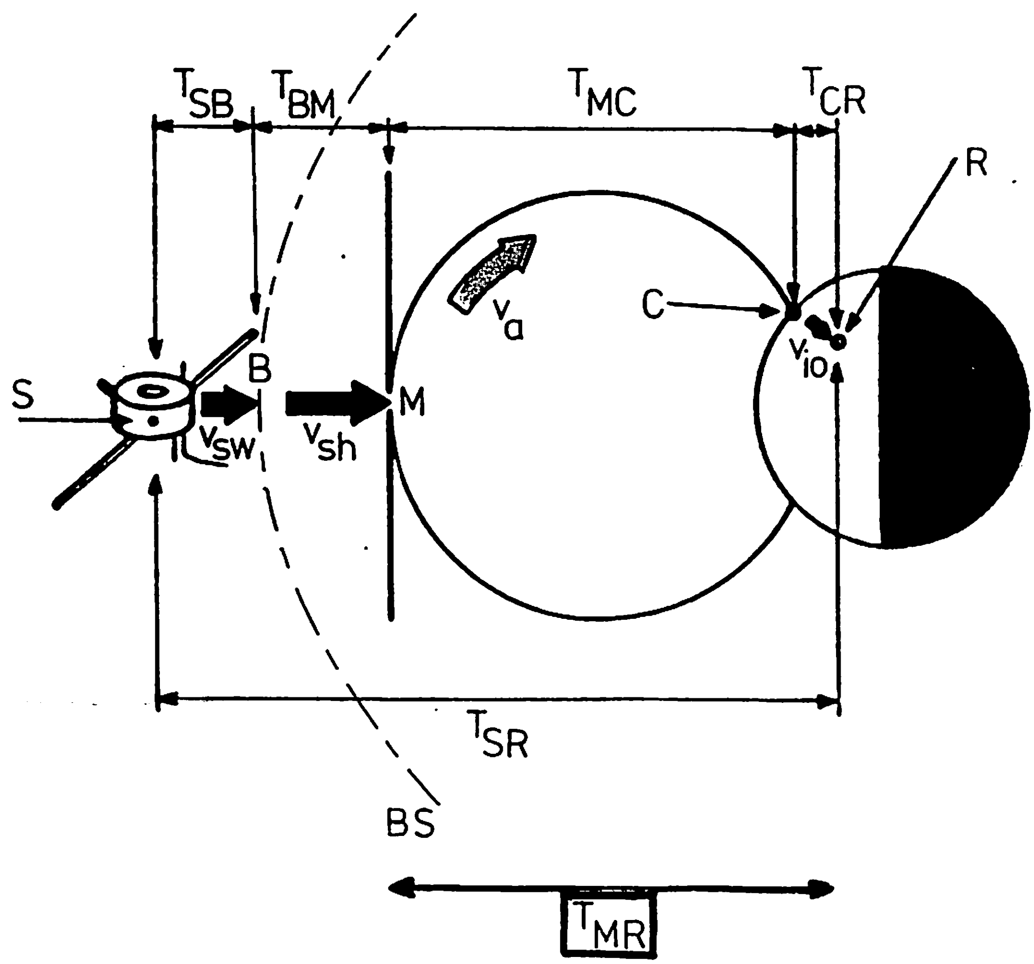

Lockwood et al., 1986

EISCAT SCIENTIFIC
ASSOCIATION
Headquarters
P.O. Box 812
S-981 28 KIRUNA, Sweden
Phone +46-980-79150/79153
Telex 8778 EISSWE S
Fax +46-980-79161

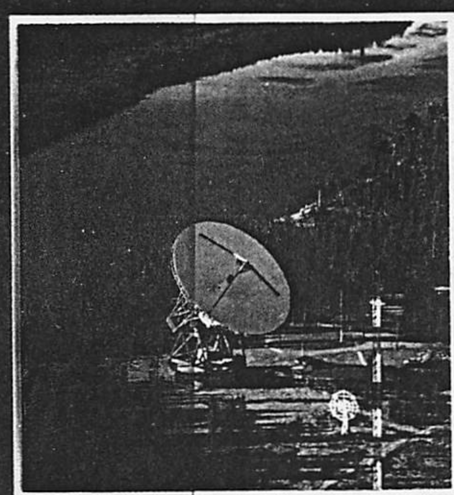

EISCAT Sodankylä
Geophysical Observatory
SF-99600 SODANKYLÄ, Finland
Phone +358-693-12462
Telex 37254 GEFSO SF
Fax +358-693-12528

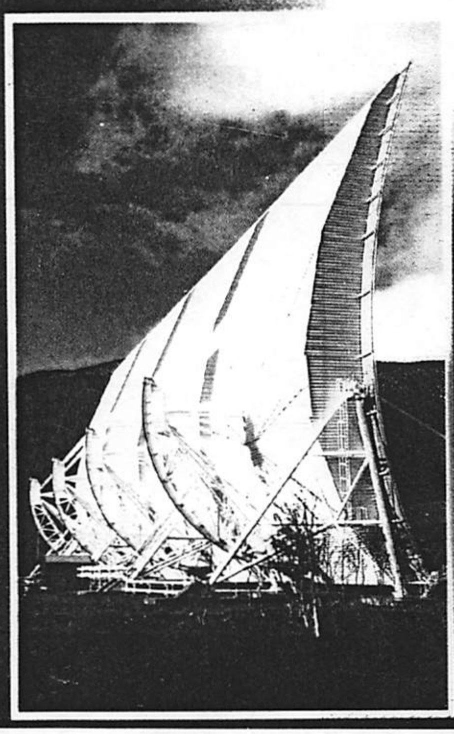

EISCAT Tromsø
Ramfjordmoen
N-9027 RAMFJORDBOTN, Norway
Phone +47-83-92166/92169
Telex 64455 EISNO N
Fax +47-83-92380

EISCAT Kiruna
Swedish Institute of Space Physics
P.O. Box 812
S-981 28 KIRUNA, Sweden
Phone +46-980-79150/79136
Telex 8754 IRF S
Fax +46-980-79050

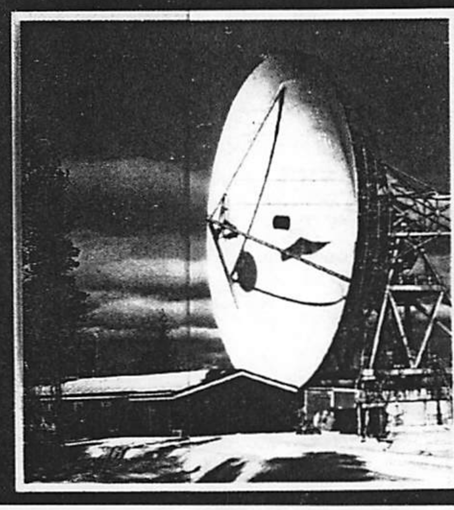

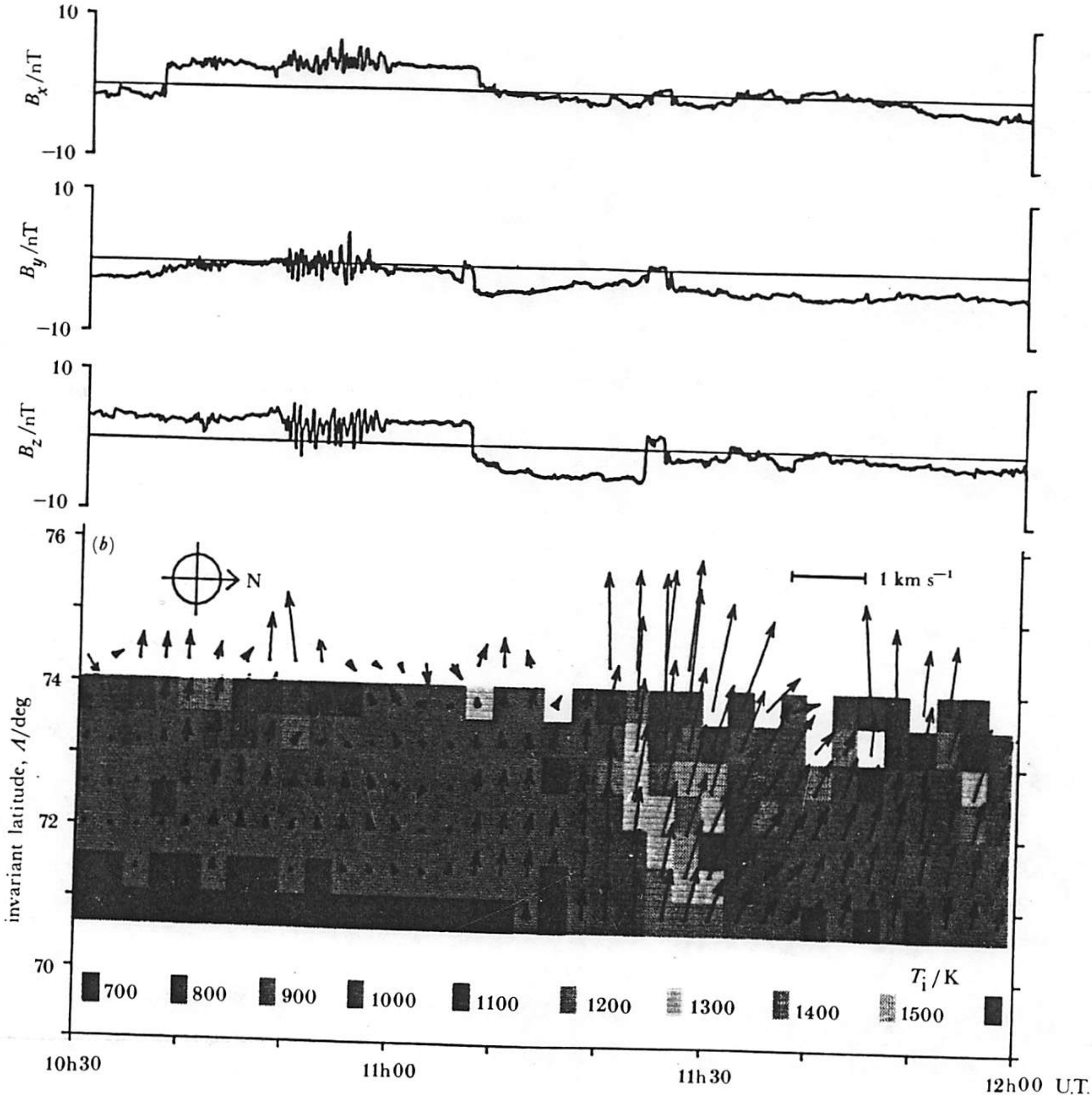

FIGURE 2. Example of an observed ionospheric response to a southward turning of the IMF (27 October 1984). (*a*) The sunward, dawnward and northward components of the IMF in GSM coordinates (B_x, B_y and B_z, respectively), observed by *AMPTE-UKS* when located immediately sunward of the Earth's bow shock. (*b*) The simultaneous observations by the EISCAT radar. The flow vectors have been rotated through 90° to avoid congestion of the plot; hence northward flow is shown by vectors directed to the right of the figure and westward flow by vectors directed upward (i.e. the vectors are in the direction of the electric field). The vectors are superimposed on a colour plot of two-minute averages of the ion temperature, T_i. (From Willis *et al.* 1986.)

Etemadi et al., 1988a;b

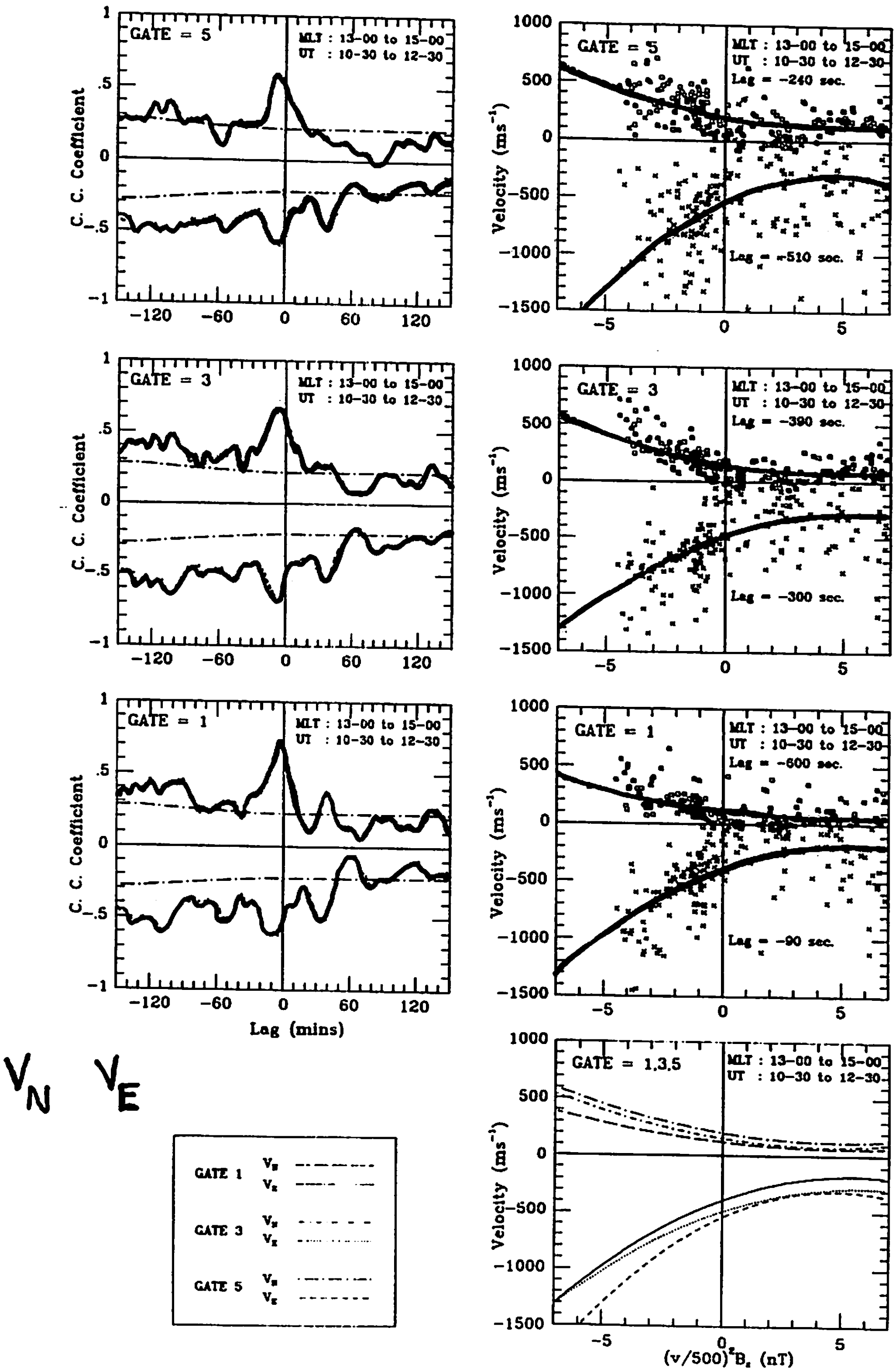

FIG. 4c. AS FOR FIG. 4a EXCEPT FOR THE LOCAL TIME INTERVAL FROM 13:00 TO 15:00 M.L.T.

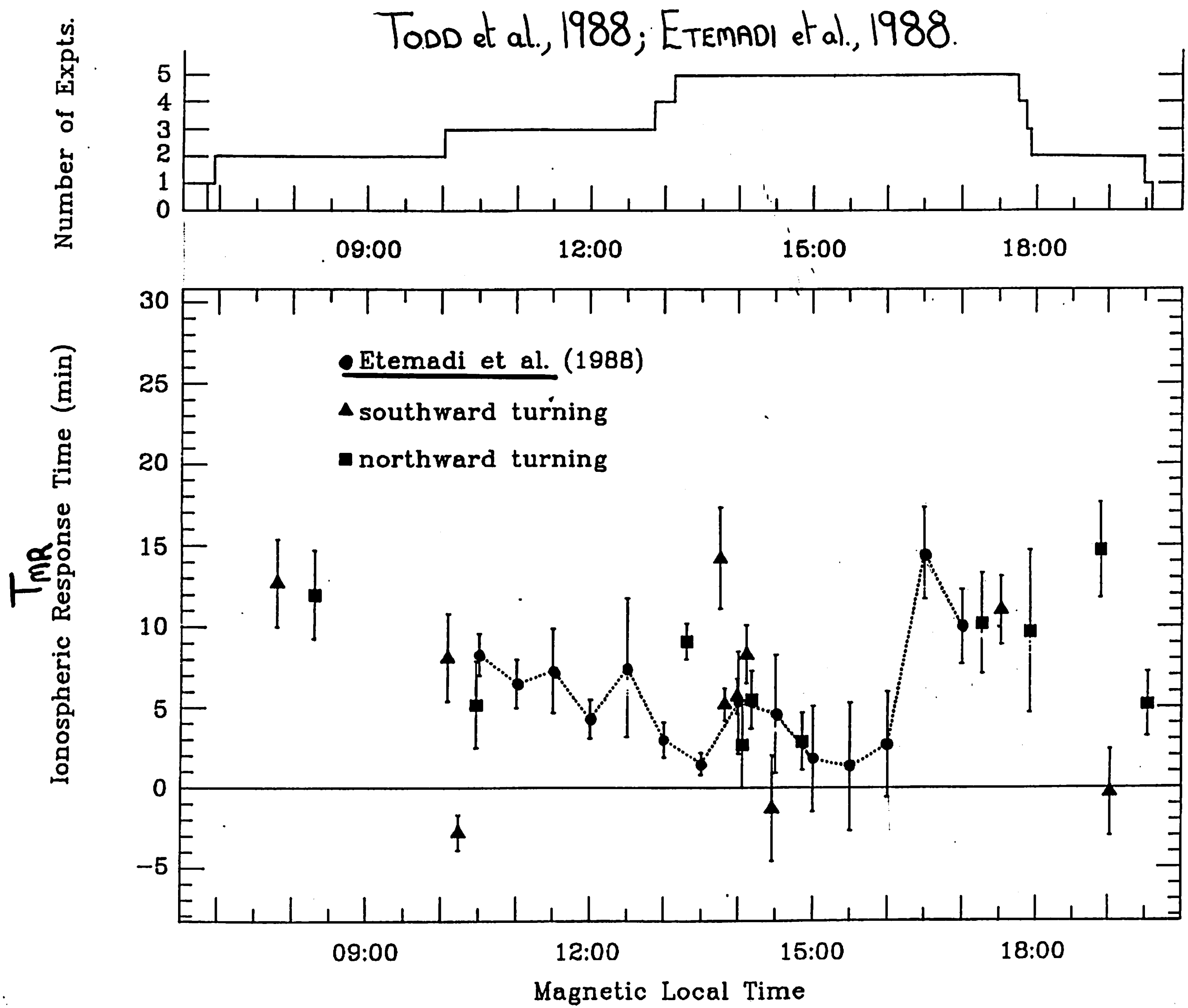
Todd et al., 1988; Etemadi et al., 1988.
Number of Expts.
09:00
12:00
15:00
18:00
Etemadi et al. (1988)
southward turning
northward turning
T_{MR}
Ionospheric Response Time (min)
Magnetic Local Time

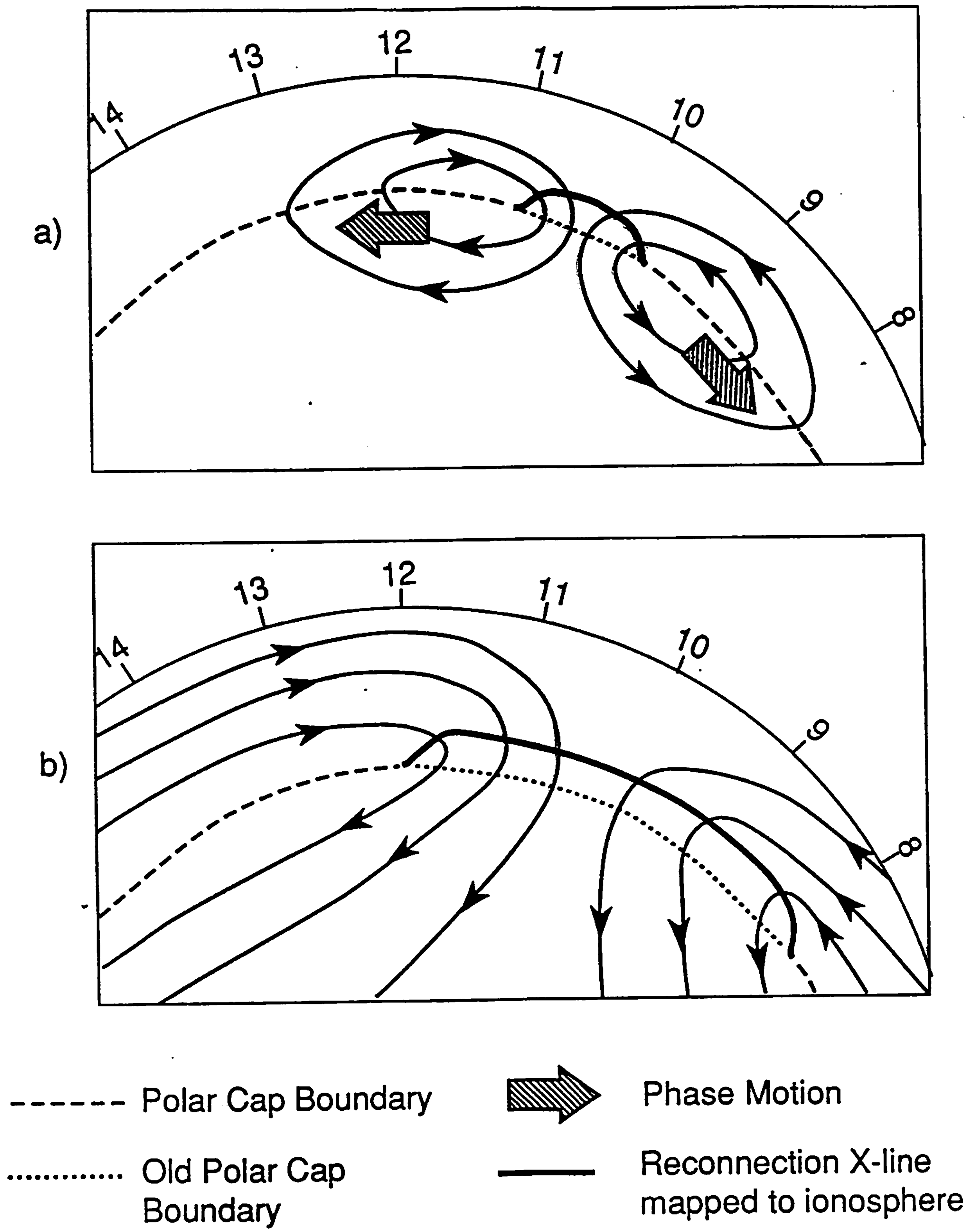

Phase velocity initially ~ 10 km s⁻¹, falls with MLT from ~12 hrs.

Directly Observed by Lockwood et al. (1986)
Saunders et al. (1992)

"Adiaroic" segments of open/closed boundary

(meaning "not flowing across") - Introduced by Siscoe and Huang (1985).

Open/closed boundary, in its OWN REST FRAME

$\bar{v} = (\bar{E} \times \bar{B})/B^2$

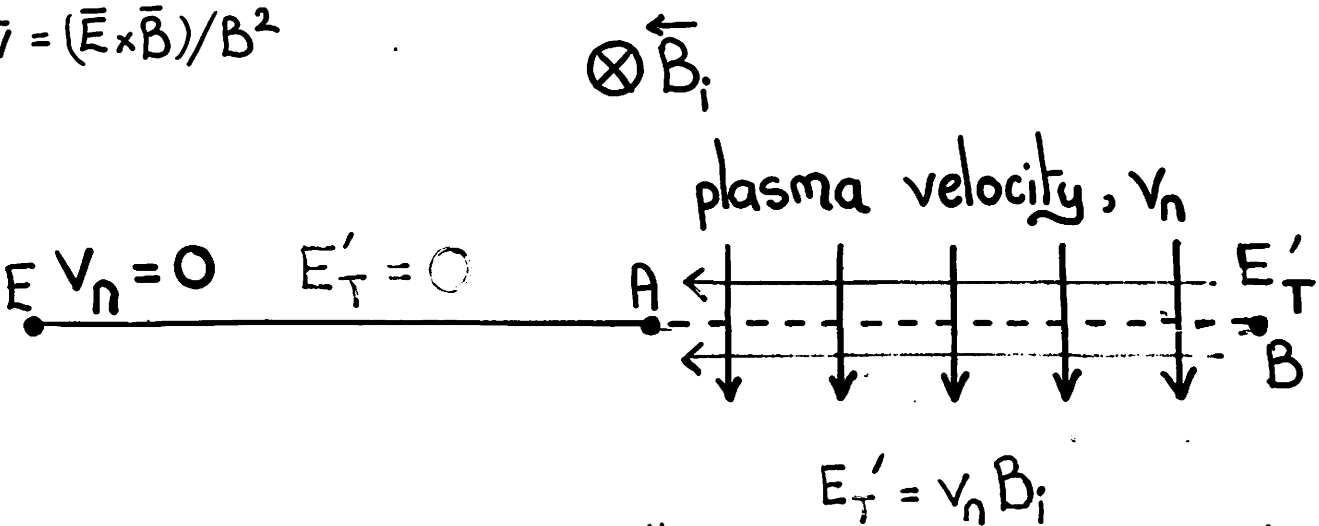

Adiaroic segment, EA

Voltage, $\phi'_{EA} = \int_E^A E'_T \, dl = 0$

Merging gap, AB

(Ionospheric projection of reconnection X-line)

Voltage, $\phi'_{AB} = \int_A^B E'_T \, dl \neq 0$

By Faraday's Law, ϕ' is a flux transfer rate

ϕ'_{AB} = voltage across corresponding reconnection X-line

Moving Open/Closed Boundary with speed V_b in EARTH'S FRAME (because polar cap expands/contracts)

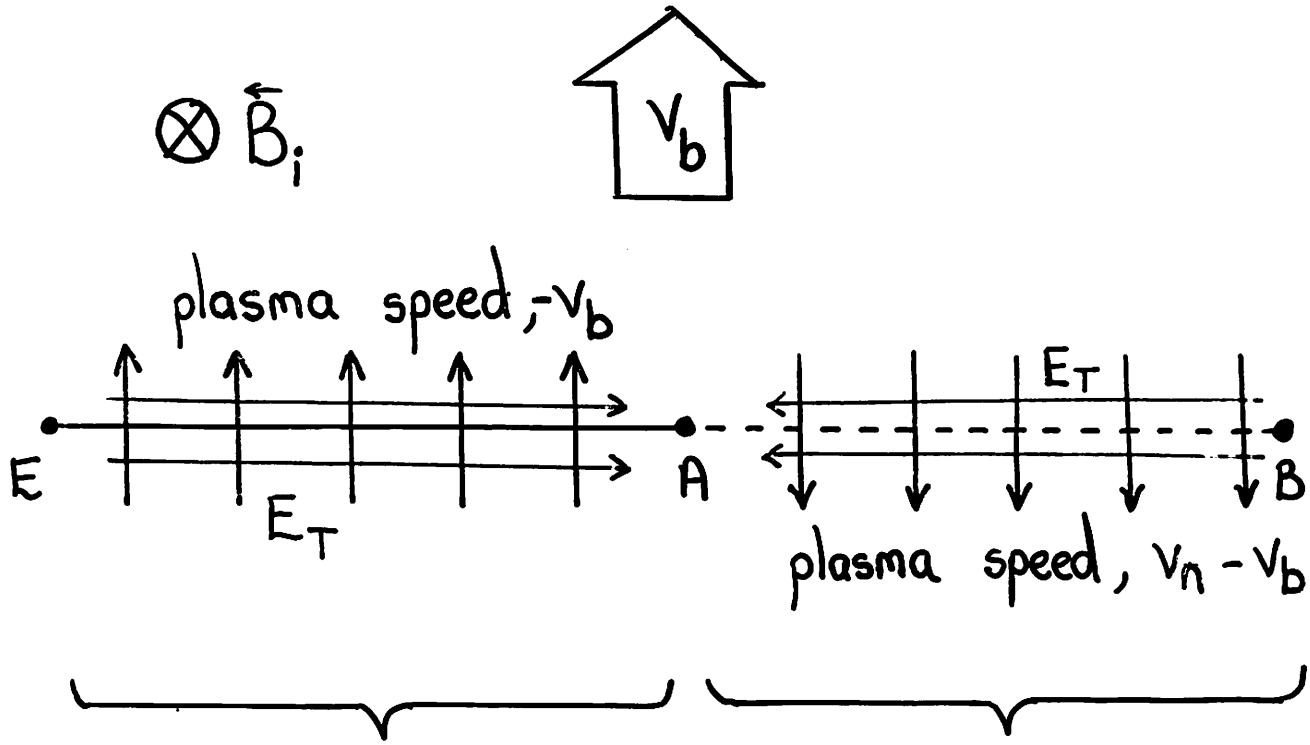

Adiaroic Segment, EA	Merging gap AB
$E_T = -V_b B_i$	$E_T = (V_n - V_b) B_i$
Voltage, $\phi_{EA} = \int_E^A -V_b B_i \, dl$	Voltage, $\phi_{AB} = \int_A^B (V_n - V_b) B_i \, dl$
	$= \phi'_{AB} - \int_A^B V_b B_i \, dl$

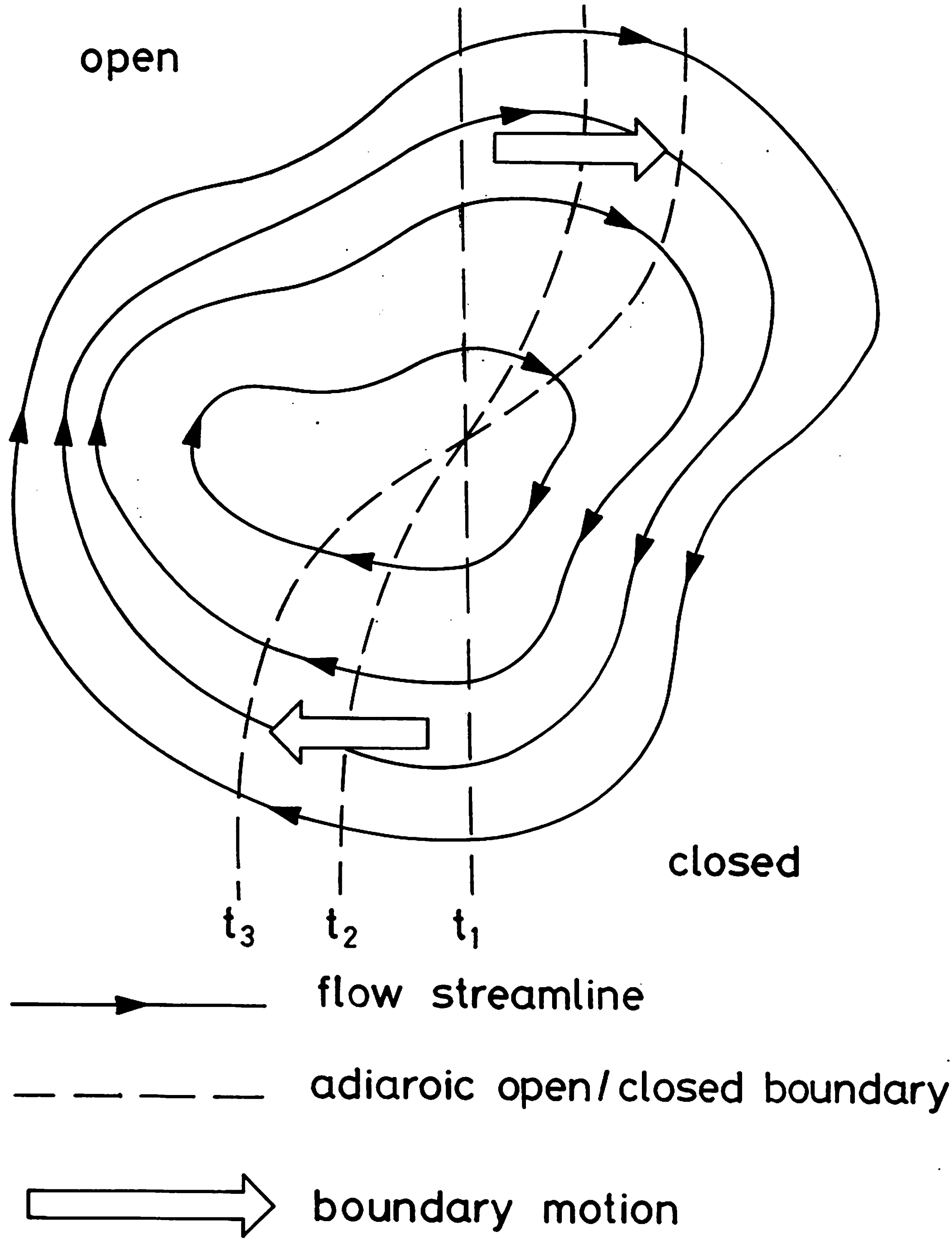

Lockwood and Cowley (1992)

Faraday's Law applied to polar cap:

$$\oint_{pc} \underline{E}\cdot d\underline{l} = \partial(B_i A_{pc})/\partial t = \boxed{B_i\, \partial A_{pc}/\partial t = \Phi_d - \Phi_n}$$

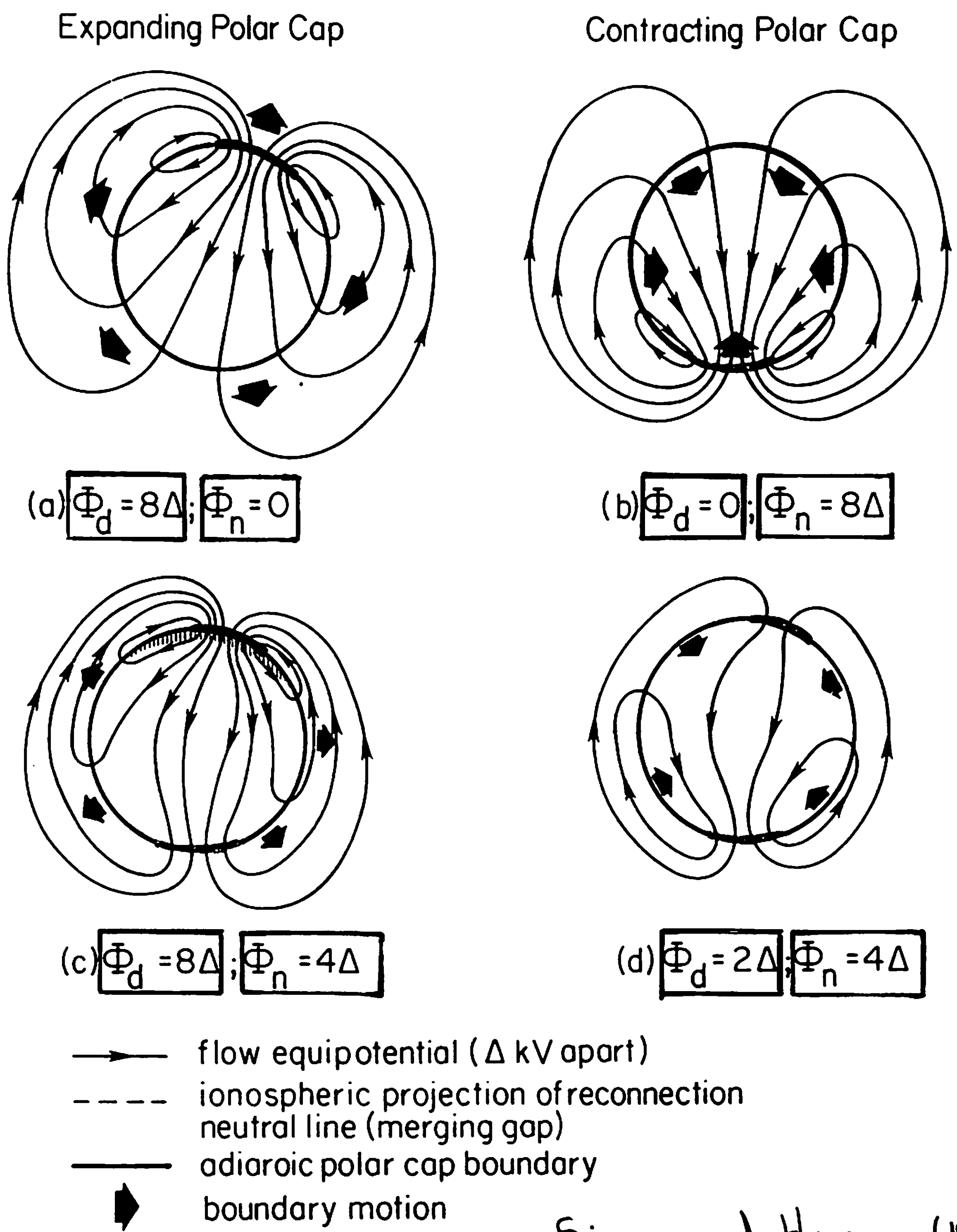

Siscoe and Huang (1985)
Lockwood and Cowley (1988)
Lockwood et al. (1990)
Russell (1972)

Zero-flow equilibrium configurations

(Cowley and Lockwood, 1992)

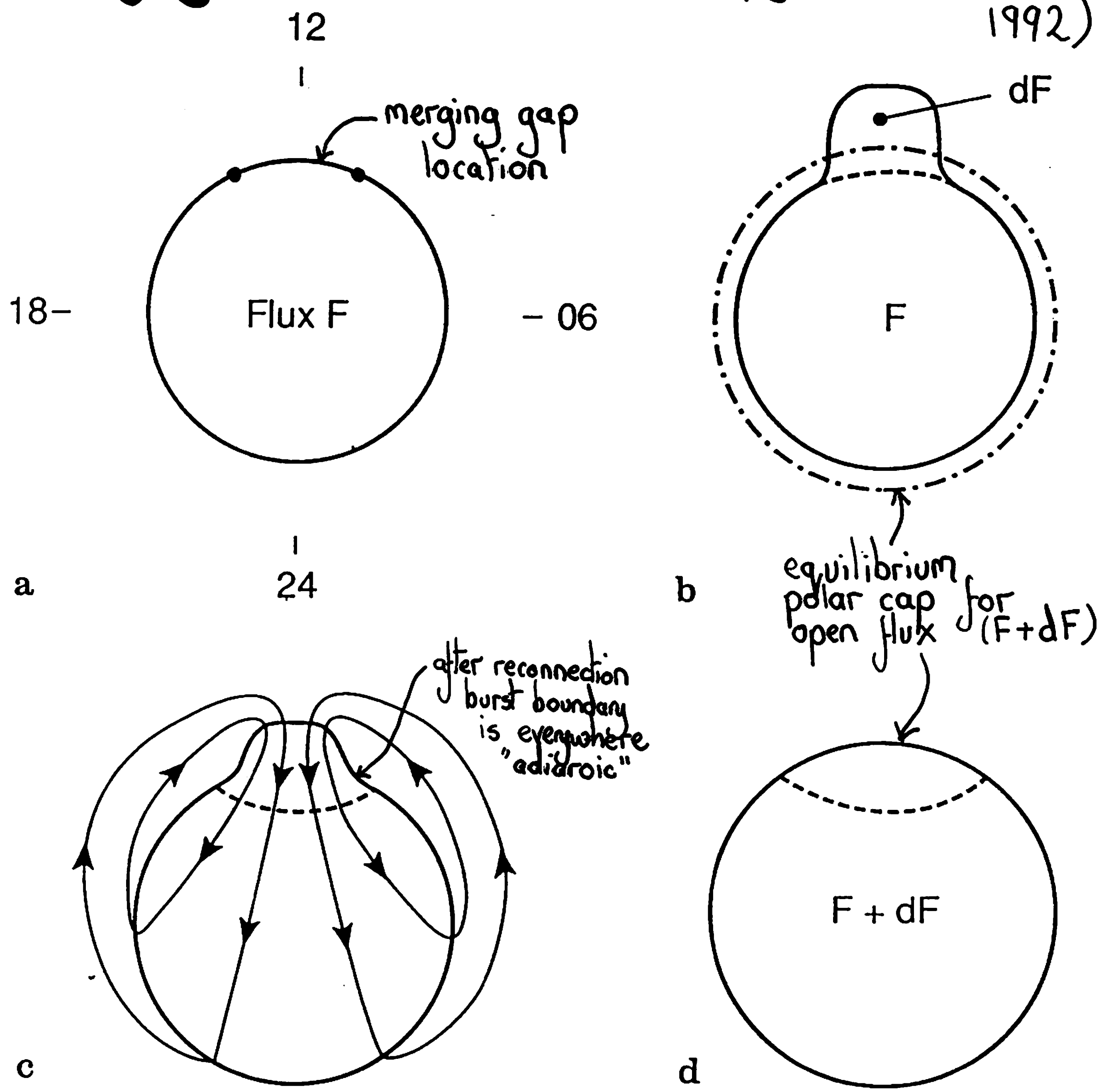

NB:

- equilibrium configurations only assumed circular here for illustrative purposes
- in reality, flux dF will not be opened instantaneously
- Lockwood et al. (1990) estimate $dF/F \lesssim 0{\cdot}03$

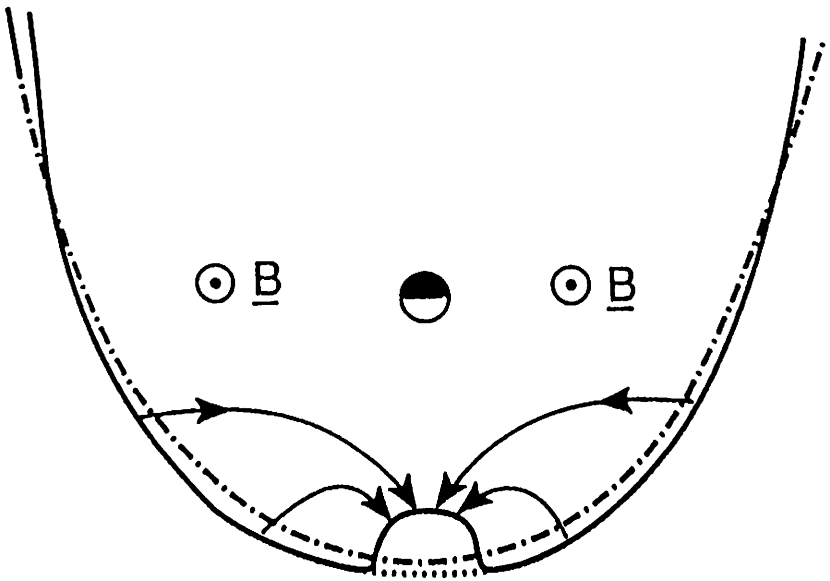

● a
In the equatorial magnetosphere

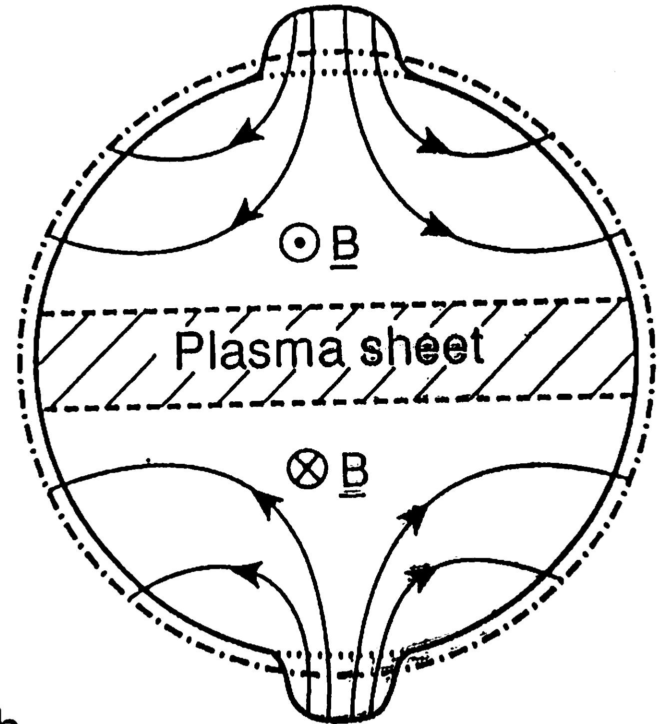

● b
In the geomagnetic tail

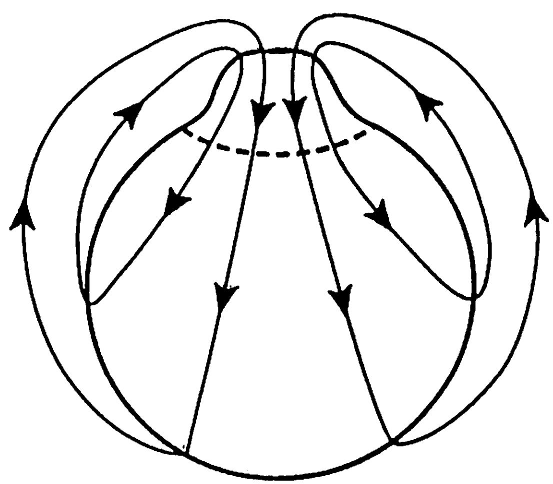

● c
In the polar ionosphere

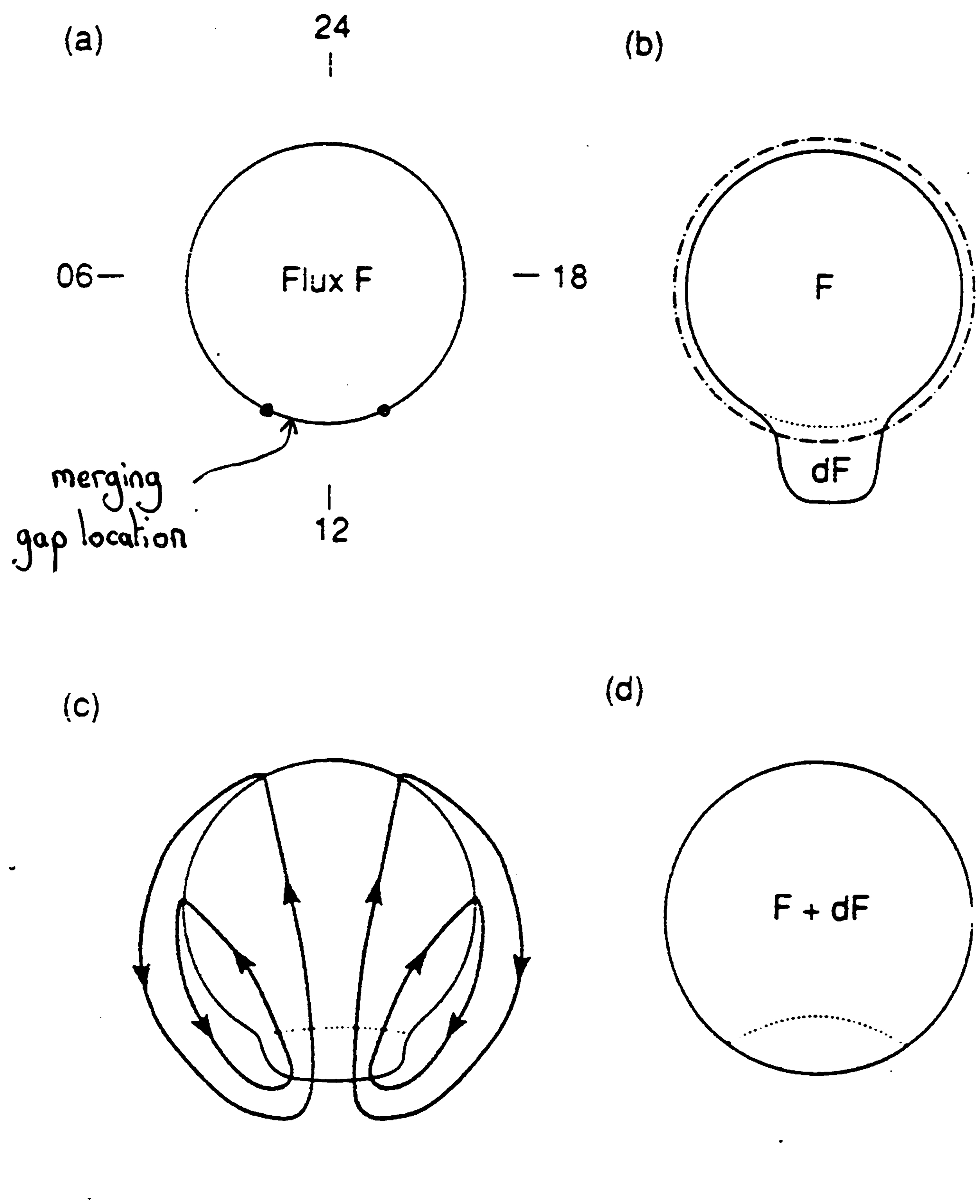
(a)
24
06—
Flux F
— 18
merging gap location
12
(b)
F
dF
(c)
(d)
F + dF

Zero-flow equilibria

(Introduced by Cowley and Lockwood, 1992)

(a)

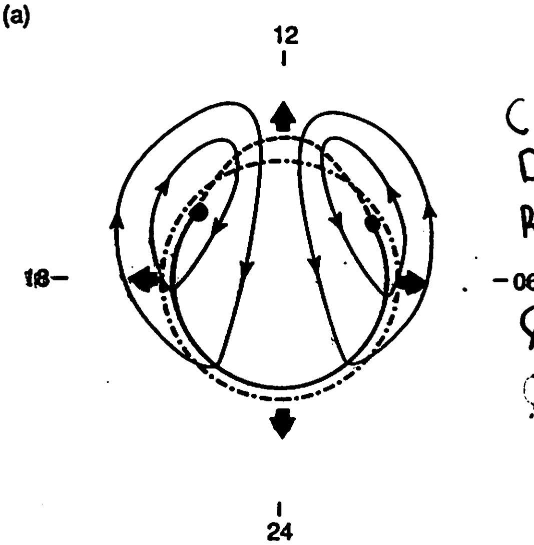

Continuous Dayside Reconnection

$\phi_d > 0$

$\phi_n = 0$

(b)

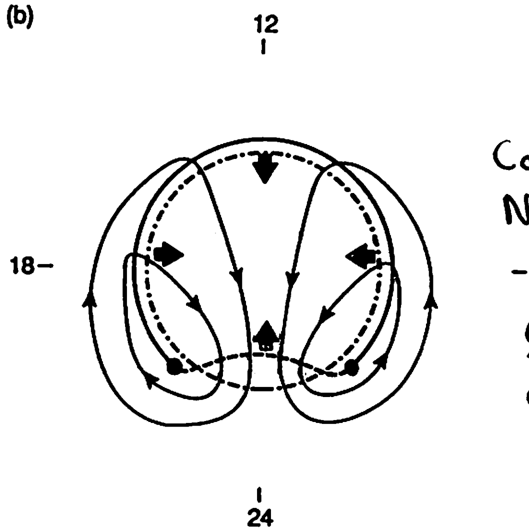

Continuous Nightside Reconnection

$\phi_d = 0$

$\phi_n > 0$

NB. Average over a long (several days) time scale and $\frac{d}{dt} A_{pc} = 0$, i.e. $\phi_d = \phi_n$

$\therefore$ Long term averages are steady-state models.

(c)

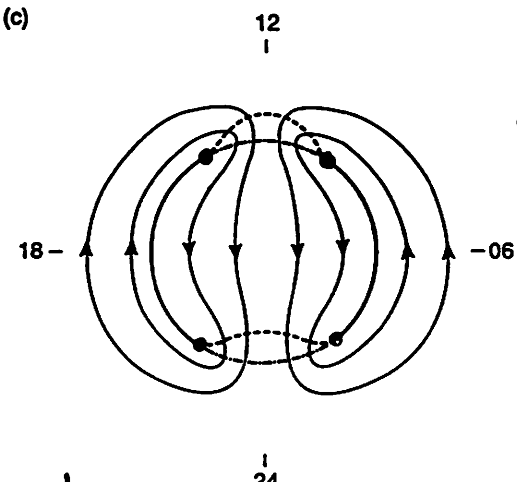

Steady State

$\phi_d = \phi_n$

$\left.\begin{matrix} \bullet & \bullet \\ \bullet & \bullet \end{matrix}\right\}$ ends of $\left\{\begin{matrix} \text{dayside} \\ \text{nightside} \end{matrix}\right\}$ merging gaps

Northward IMF Substorms

(a)

Steady-State with $\phi_d' = \phi_n = 0$

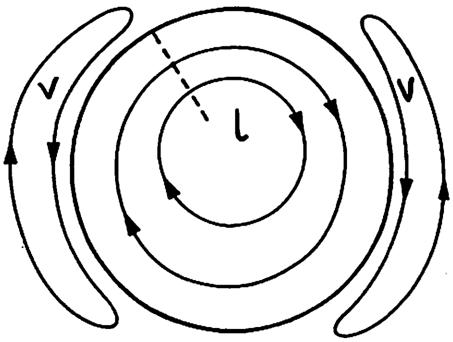

lobe circulation cell (l) due to reconfiguration of already open field lines.

v are viscously driven cells.

(b)

$\phi_d' = 0$

$\phi_n' > 0$

$\phi_v > 0$

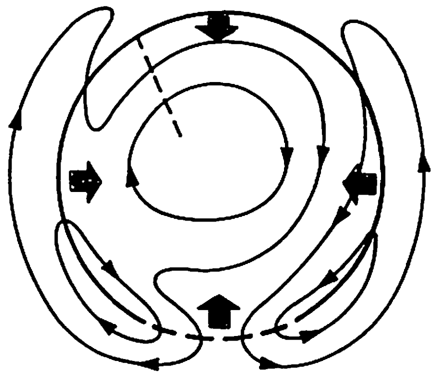

Boundary moves so lobe and viscous cells are no longer distinct

(c)

$\phi_d' = 0$

$\phi_n' > 0$

$\phi_v = 0$

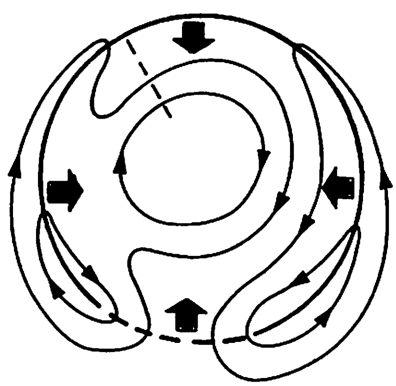

Similar pattern if no viscous interaction

——— adiaroic open / closed boundary

– – – merging gap

—►— flow streamline

➡ boundary motion

Lockwood and Cowley (1992)

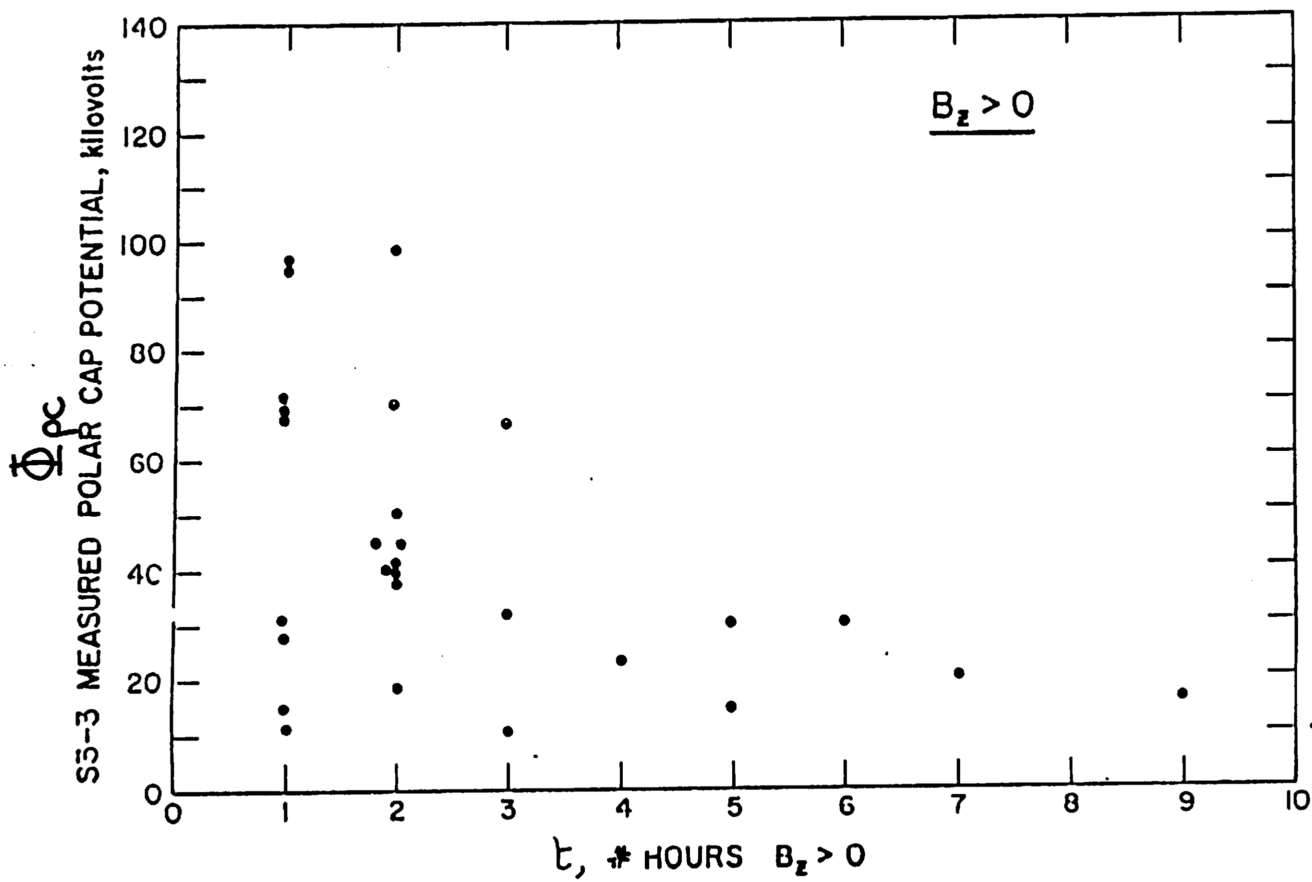

Fig. 6. The cross polar cap potential during periods when B_z^{IMF} was northward versus the number of hours previous to the measurement of the polar cap potential that B_z^{IMF} was northward.

$\leftarrow \phi_v \sim 10$kV?

Initial Range of Φ_{pc} large, because of range of Φ_n

After ~9 hrs Φ_n is small $\Phi_{pc} \sim \phi_v$

$\phi_d = 0$ for $t \geq 0$

range of Δ and ϕ_n, but $\Phi_{pc} \sim \Phi_n/2$ for $t \geq 0$

ϕ_n decays over $t \sim 10$hrs

I.S. radar data + magnetometer observations give global convection "snapshots" by the AMIE technique:-

Knipp et al. (Geophys. Res. Lett., 1991)

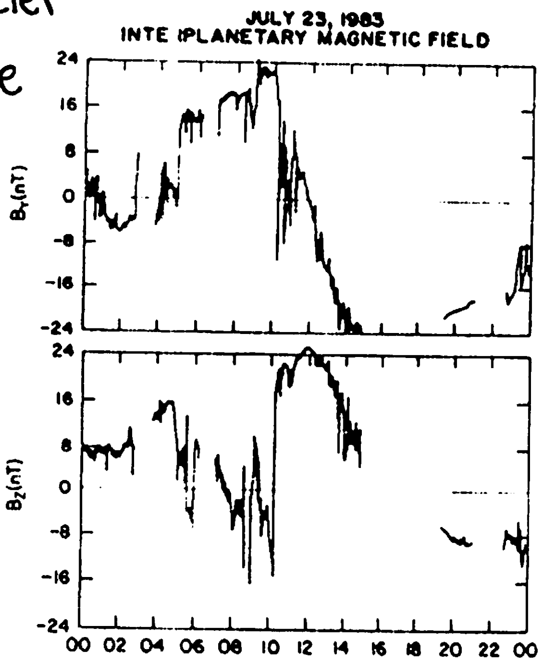

1. IMP-8 IMF data (GSM coordinates) for 23 July 1983.

Northward IMF turning
10:15 UT at IMF-8
~10:25 UT at magnetopause

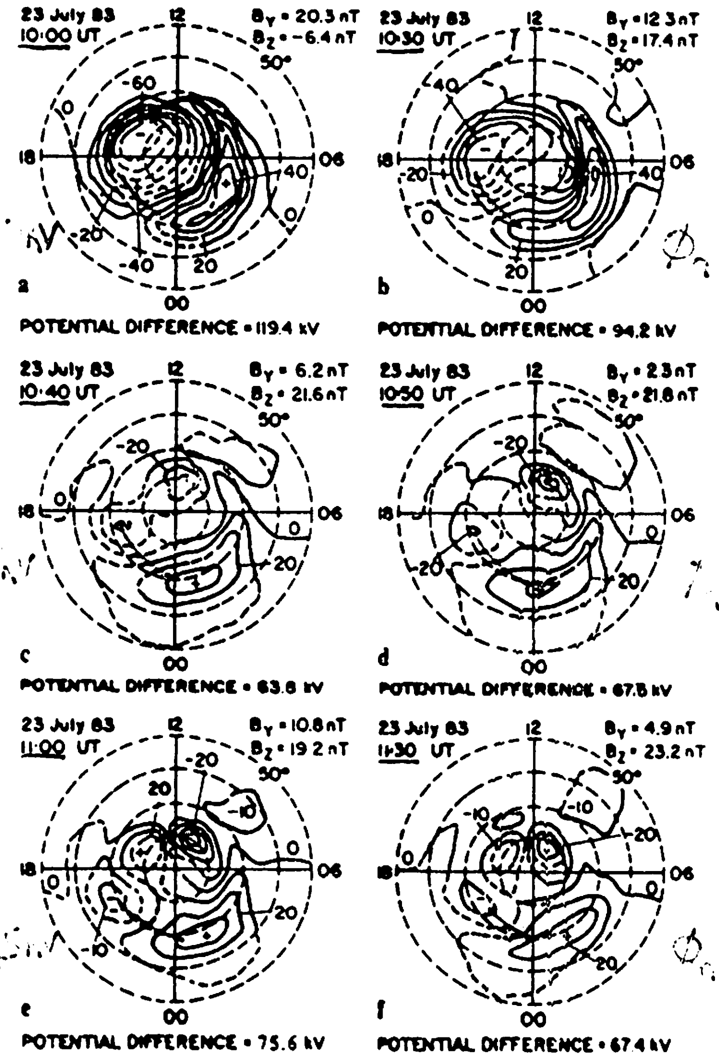

$\Phi_n \sim 60$ kV

$\Phi_n \sim 35$ kV

Fig. 3. Fitted electric potential patterns for selected times between 1000 UT and 1130 UT on 23 July 1983. The contour interval is 10 kV. The IMF values are shown at the upper right. In regions where the uncertainty in the large-scale electric field is 50% or greater the contours are dashed.

Φ_d and dayside flow decay in ~10min

Φ_n and nightside flow decay in several hours

1991)

March 22, 1979 Substorms
(CDAW 6)

McPherron and Manka (1985)

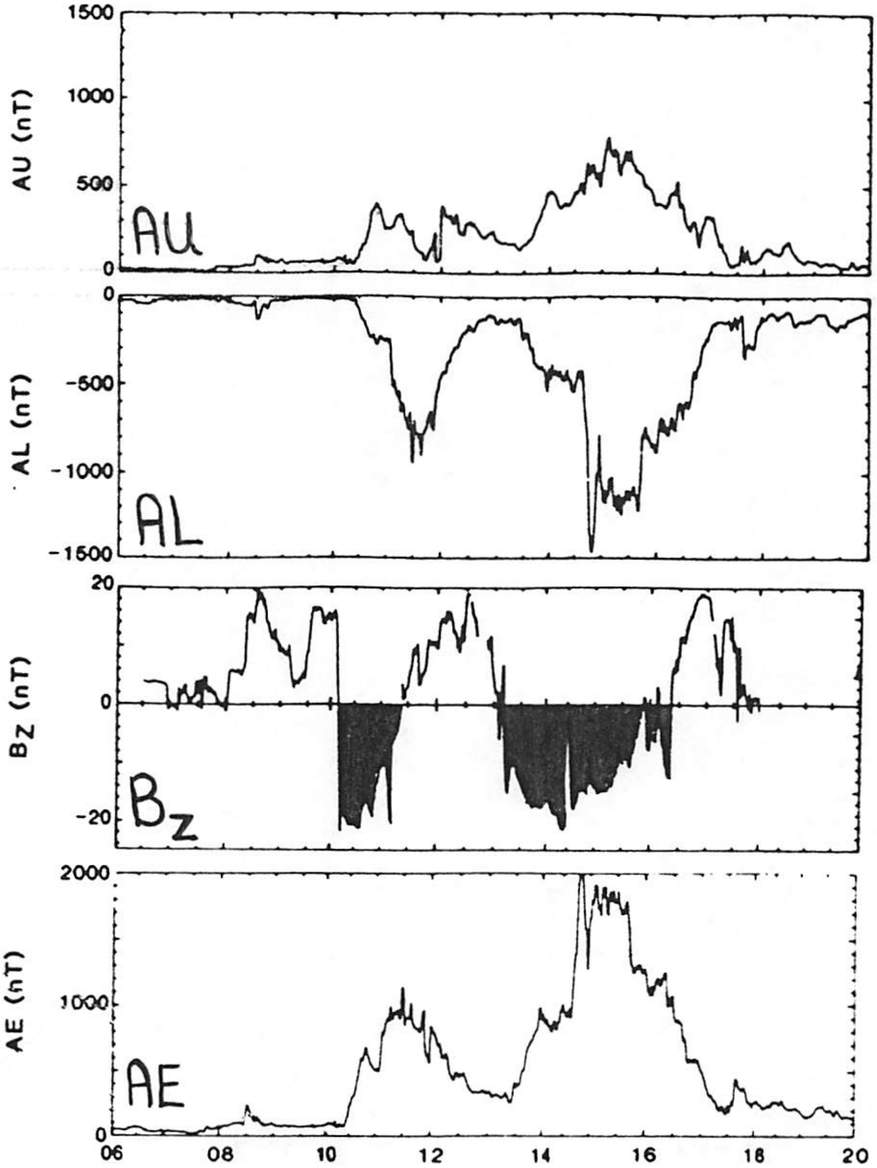

Holzer et al. (1986)

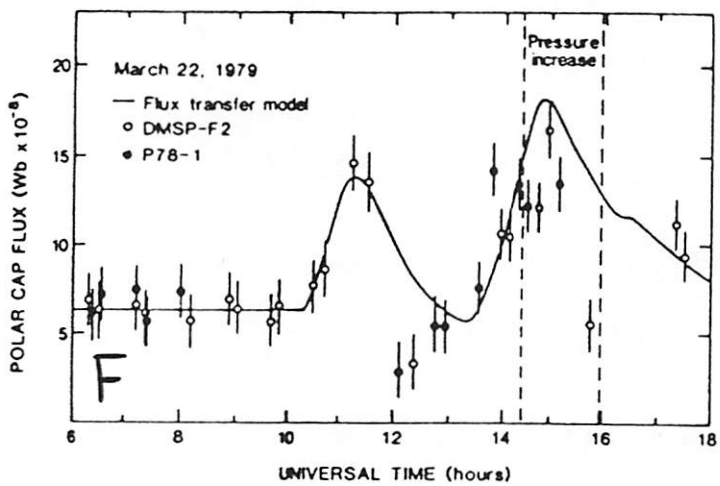

c.f. Kamide and Baumjohann (1985)

KRM method
CDAW-6
22 March 1979

ELECTRIC POTENTIAL

Growth phase

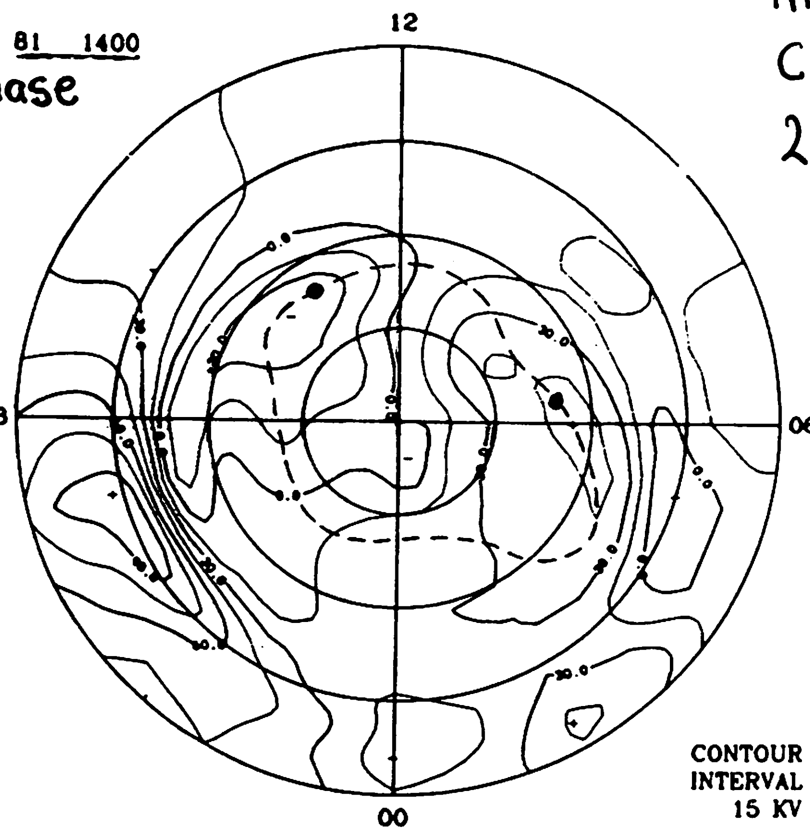

ELECTRIC POTENTIAL

Expansion phase

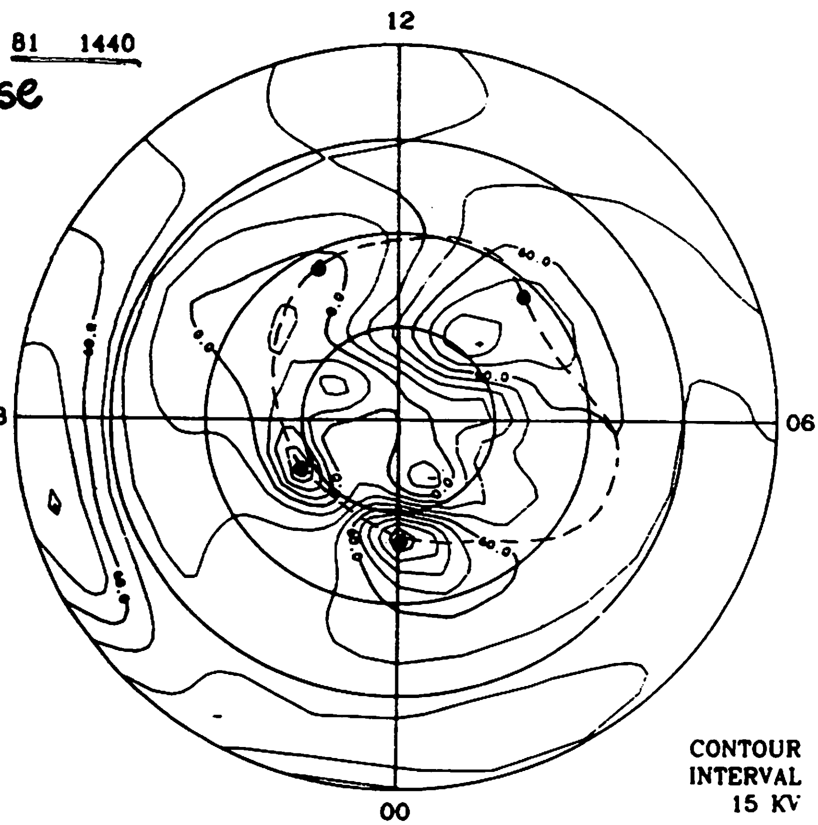

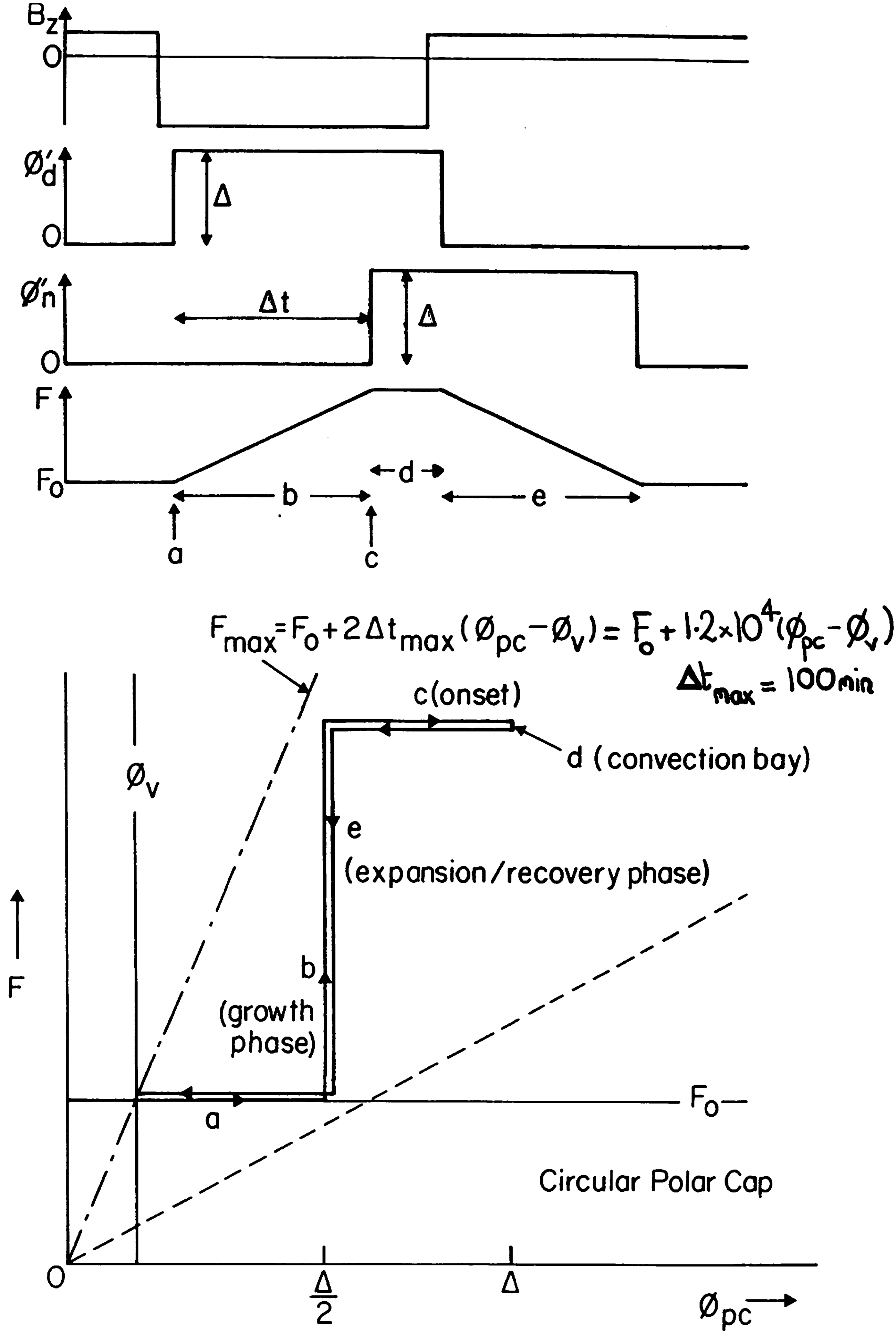

B_z
O
ϕ'_d
Δ
O
ϕ'_n
Δt
Δ
O
F
F_o
d
b
e
a
c
$F_{max} = F_o + 2\Delta t_{max}(\phi_{pc} - \phi_v) = F_o + 1.2\times10^4(\phi_{pc} - \phi_v)$
$\Delta t_{max} = 100$ min
c (onset)
d (convection bay)
ϕ_v
e
(expansion/recovery phase)
F
b
(growth phase)
F_o
a
Circular Polar Cap
O
$\frac{\Delta}{2}$
Δ
ϕ_{pc}

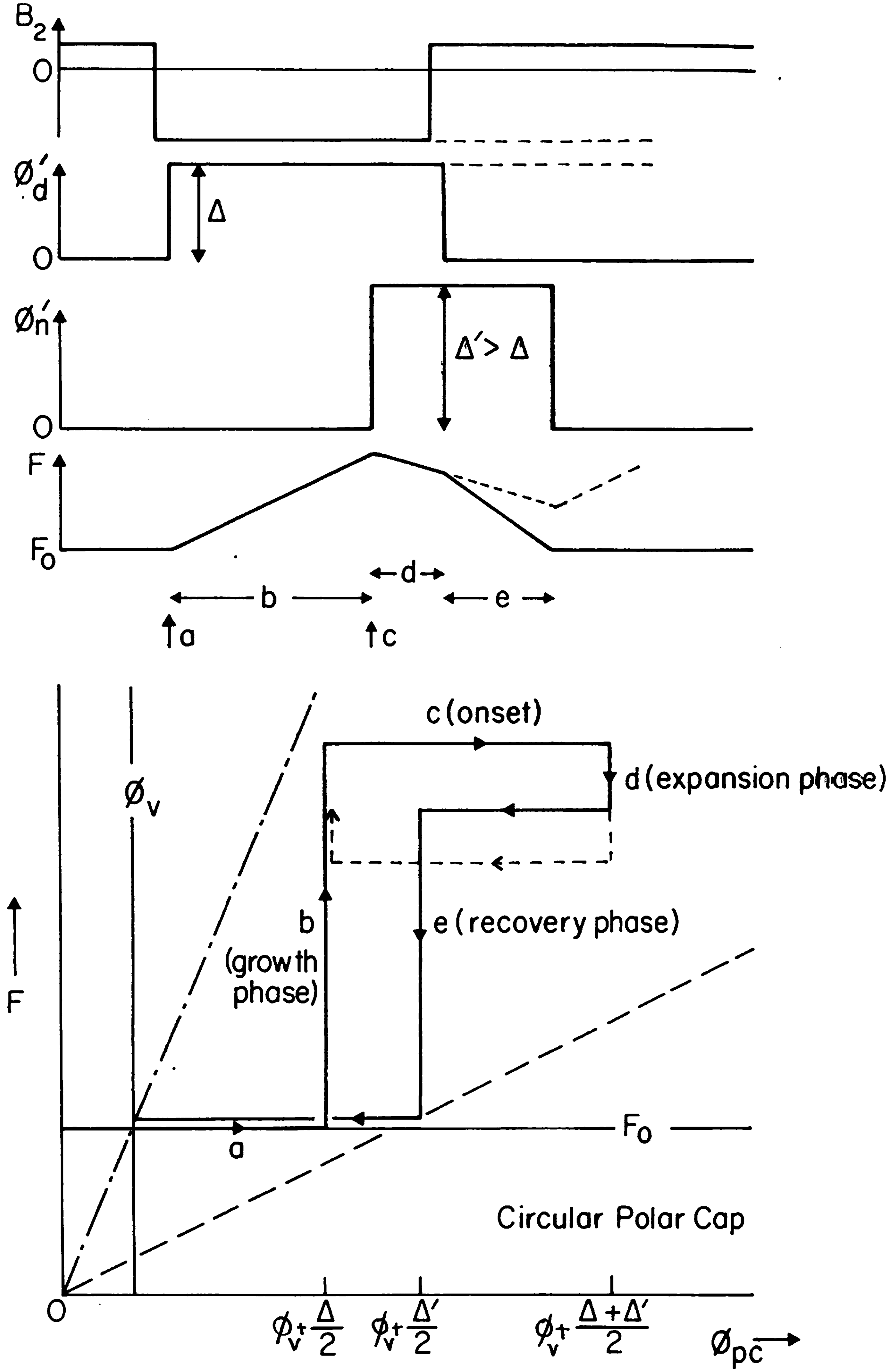

Lockwood and Cowley (1992)

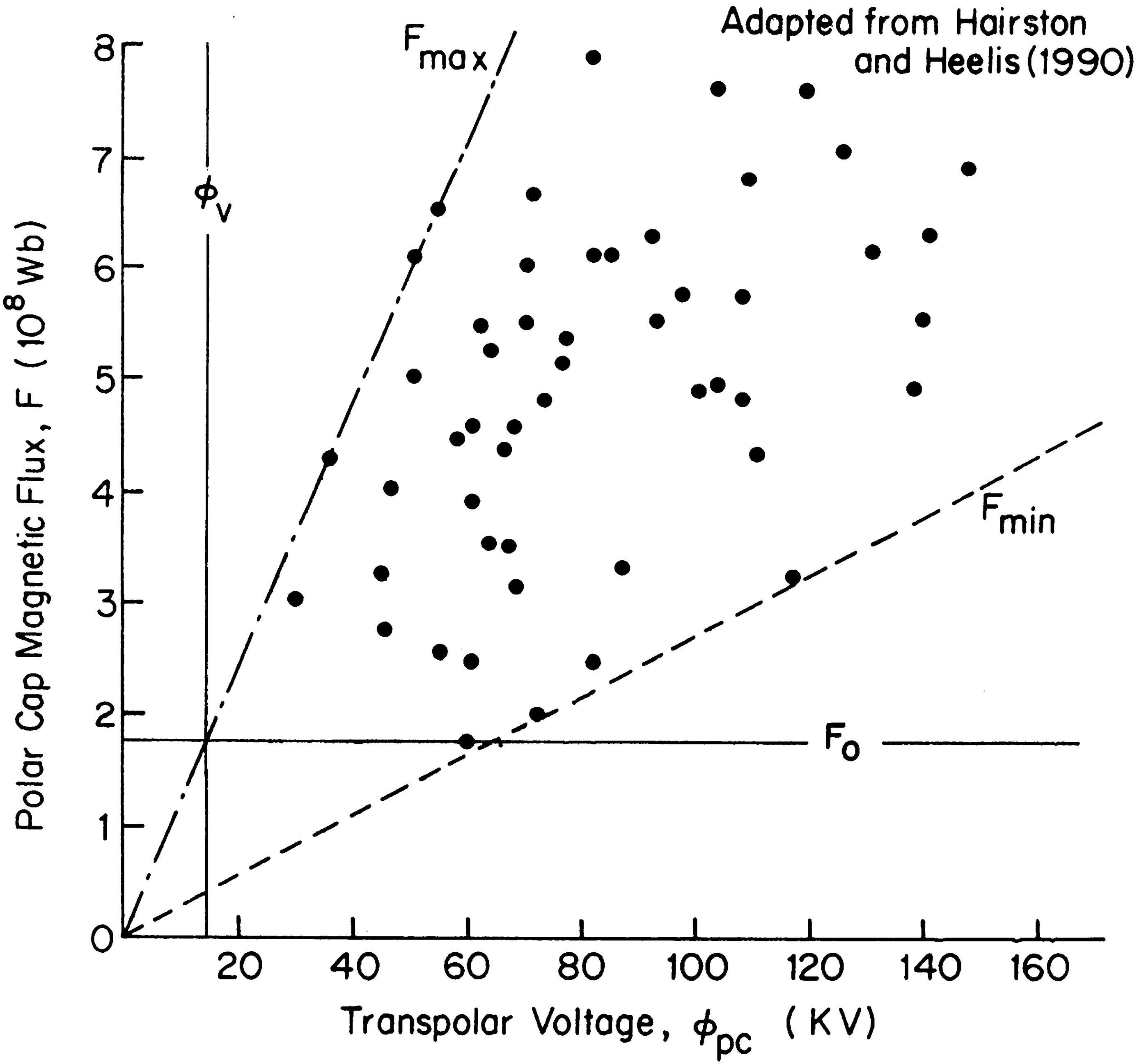
Adapted from Hairston and Heelis (1990)
F_{max}
ϕ_v
F_{min}
F_0
Polar Cap Magnetic Flux, F (10^8 Wb)
Transpolar Voltage, ϕ_{pc} (KV)
0
1
2
3
4
5
6
7
8
20
40
60
80
100
120
140
160

Summary

- Comparison of ionospheric transpolar voltage with voltage across LLBL shows convection is predominantly driven by reconnection
- Explains B_y and B_z effects on convection
- Consideration of length of magnetotail and variability of IMF B_z shows steady-state is exceptional, in anything other than an average sense
- ALL empirical models of convection and MOST conceptual ones assume steady state
- Electric fields DO NOT map from the magnetopause to the ionosphere in non-steady conditions
- In non-steady cases flow streamlines cross non-reconnecting (but moving) open/closed boundary
- Average convection is the sum of 2 flow patterns driven by dayside and nightside reconnection
- Much viscous-like interaction is in fact residual nightside reconnection
- Transpolar voltage and polar cap size vary in a regular way during the substorm cycle